Water Science & Technology

Water Science & Technology Vol 87 No 3, 761 doi: 10.2166/wst.2023.009

Review on the degradation of chlorinated hydrocarbons by persulfate activated with zero-valent iron-based materials

Zhiguo Chen[a,b], Wenqing Cao[b], He Bai[b], Rong Zhang[a,b], Yiyun Liu[b], Yan Li[b], Jingpeng Song[b], Juncheng Liu[b,*] and Gengbo Ren[c]

[a] School of Chemical Engineering and Technology, Tianjin University, Tianjin 300072, China
[b] Tianjin Huakan Environmental Protection Technology Co., Ltd, Tianjin 300170, China
[c] School of Energy and Environment Engineering, Hebei University of Technology, Tianjin 300401, China
*Corresponding author. E-mail: 397055891@qq.com

ABSTRACT

Chlorinated hydrocarbons (CHCs) are often used in industrial processes, and they have been found in groundwater with increasing frequency in recent years. Several typical CHCs, including trichloroethylene (TCE), 1,1,1-trichloroethane (TCA), carbon tetrachloride (CT), etc., have strong cytotoxicity and carcinogenicity, posing a serious threat to human health and ecological environment. Advanced persulfate (PS) oxidation technology based on nano zero-valent iron (nZVI) has become a research hotspot for CHCs degradation in recent years. However, nZVI is easily oxidized to form the surface passivation layer and prone to aggregation in practical application, which significantly reduces the activation efficiency of PS. In order to solve this problem, various nZVI modification solutions have been proposed. This review systematically summarizes four commonly used modification methods of nZVI, and the theoretical mechanisms of PS activated by primitive and modified nZVI. Besides, the influencing factors in the engineering application process are discussed. In addition, the controversial views on which of the two ($SO_4^{\cdot-}$ and ·OH) is dominant in the nZVI/PS system are summarized. Generally, $SO_4^{\cdot-}$ predominates in acidic conditions while ·OH prefers neutral and alkaline environments. Finally, challenges and prospects for practical application of CHCs removal by nZVI-based materials activating PS are also analyzed.

Key words: chlorinated hydrocarbons, nZVI modification, persulfate, zero-valent iron

HIGHLIGHTS

- The mechanism of zero-valent iron-based activated persulfate was systematically summarized.
- The dominant free radical in the process of CHCs degradation by modified zero-valent iron activated persulfate was summarized and analyzed.
- Various influencing factors of zero-valent iron activated persulfate were analyzed.

GRAPHICAL ABSTRACT

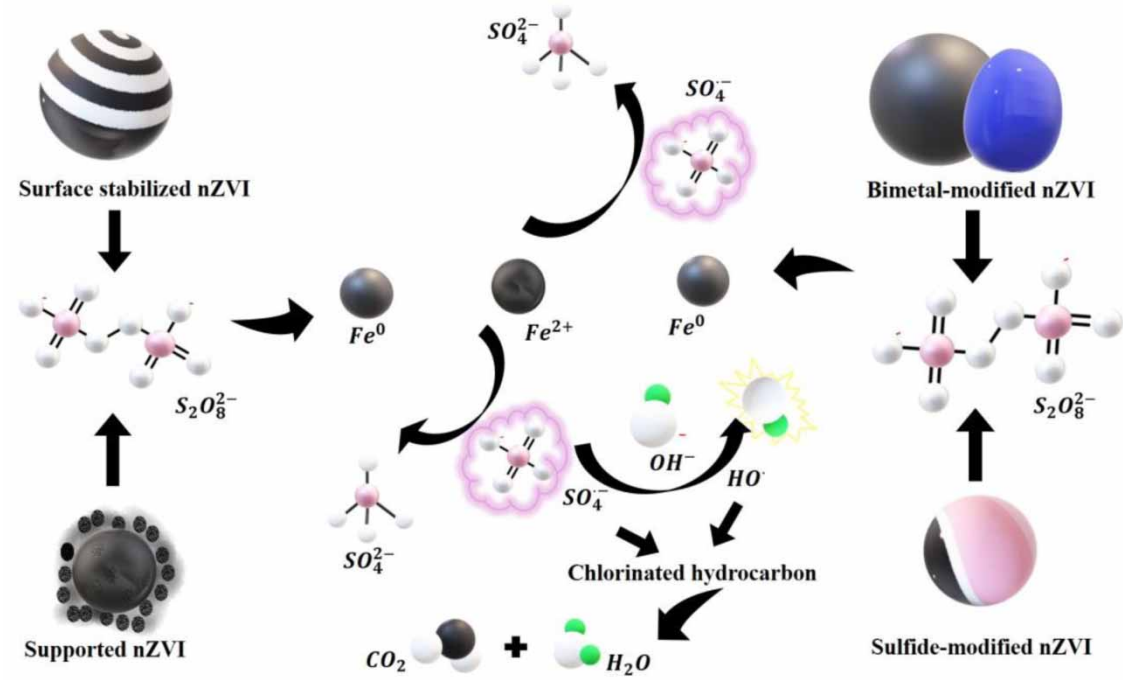

1. INTRODUCTION

Chlorinated hydrocarbons (CHCs) are an important organic solvent and chemical intermediates widely used in industrial production and human activities (Kueper *et al.* 1989). Most CHCs, such as trichloroethylene (TCE), 1,1,1-trichloroethane (TCA), and carbon tetrachloride (CT), have stable chemical properties and easily dissolve into non-polar substances. Therefore, in recent decades, CHCs have often been used as solvents, cleaners, or extractants in the pharmaceutical, chemical, and electrical engineering industries (Huang *et al.* 2014a). However, they often enter into groundwater through unreasonable discharge of industrial wastewater, accidental leakage of storage tanks, infiltration of leachate from waste storage sites, or improper leakage of toxic and hazardous chemical wastes, etc., leading to groundwater pollution and threatening human health (Aranzabal *et al.* 2014). Besides, CHCs can remain in the environment for a long time and they are not easily degraded naturally, making them to be a focus of attention in the field of environmental remediation.

Advanced oxidation processes (AOPs) have been widely studied in the field of wastewater treatment and used to degrade organic pollutants that are not easily biodegraded in industrial water (Yang *et al.* 2009). Traditional AOPs refer to oxidation technologies using hydroxyl radical (·*OH*) as the active species, including Fenton, ozone, photocatalysis, electrochemical oxidation, microwave and ultrasonic irradiation, supercritical water and wet air oxidation, and others (Pera-Titus *et al.* 2004; Choi *et al.* 2010; Capodaglio 2020). ·*OH* is one of the strongest oxidants and can unselectively oxidize almost any organic compound by the following basic pathways: radical addition, hydrogen abstraction, electron transfer, and radical combination (Afzal *et al.* 2012; Capodaglio 2020; Ma *et al.* 2022). The produced reaction chains will further lead to the generation of reactive species such as H_2O_2 and super oxides ($\cdot O_2^-$). Thus, the coexistence of multiple reactive species often occurs in the process of advanced oxidation reaction. These active species have a high redox potential, meaning that they can easily oxidize other substances (Moreira *et al.* 2017). Therefore, AOPs based on ·*OH* have been widely used in wastewater treatment. However, the application of this technology is limited to some extent by factors such as the narrow range of pH and complex operation (Gao *et al.* 2020). The disadvantages are particularly significant in the *in-situ* chemical remediation process of groundwater, causing researchers to increasingly shift their focus to persulfate (PS) systems (Ikea *et al.* 2018).

Persulfate, including peroxymonosulfate (PMS) and peroxydisulfate (PDS), generates free radicals with strong oxidation capacity through certain technical means (Oturan & Aaron 2014; Oh *et al.* 2016; Ren *et al.* 2023). PS oxidation is a promising technology based on sulfate radicals ($SO_4\cdot^-$) for degradation of organic pollutants. In fact, PS itself is relatively chemically

stable, and barely reacts with organic compounds, but it can be activated by a variety of media to realize its oxidation function, such as heat (Zhang *et al.* 2015; Zhu *et al.* 2018a), alkali (Furman *et al.* 2011), ultraviolet light (Ghauch *et al.* 2017), microwaves (Qi *et al.* 2014), and transition metals (Anipsitakis & Dionysiou 2004). $SO_4{\cdot}^-$, with strong oxidation ability, is created during the activation process. In contrast to the non-selective oxidation of $\cdot OH$, $SO_4{\cdot}^-$ is more inclined to oxidize unsaturated hydrocarbons, and its redox potential ($E_0 = 2.5 - 3.1$ V) is higher than that of $\cdot OH$ ($E_0 = 1.7 - 2.8$ V) (Wei *et al.* 2016; Yan *et al.* 2016). Meanwhile, the half-life of $SO_4{\cdot}^-$ ($t_{1/2} = 30 - 40$ μs) is much longer than $\cdot OH$ ($t_{1/2} < 1$ μs) (Olmez-Hanci & Arslan-Alaton 2013; Hu & Long 2016; Matzek & Carter 2016; Shokoohi *et al.* 2019), ensuring that it has enough time to contact with contaminants and mineralize them. Besides, it is an environmentally friendly oxidation active free radical that can degrade organic pollutants, converting itself into non-toxic SO_4^{2-} during the reaction. In addition, compared with other common oxidants, PS exhibits outstanding advantages, such as aqueous solubility, high activity, and stability, which make it be a promising oxidant for environmental remediation (Lei *et al.* 2015).

Although various studies on the degradation of organic pollutants in nano zero-valent iron (nZVI)–PS system have been reported, there are still some controversies about the mechanism of oxidation process. Besides, there is no conclusive study on the degradation of CHCs by zero-valent iron-based materials and PS. The main purpose of this paper is to summarize the PS activation pathways by nZVI and modified nZVI to analyze the degradation mechanism of CHCs. Meanwhile, several common factors influencing the activation process are also summarized. Finally, the application prospects of nZVI and modified nZVI to degrade CHCs are analyzed, in order to provide reference for related engineering applications.

2. MECHANISMS OF PS ACTIVATED BY TRANSITION METALS

The advantage of transition metals activating PS is that the reaction condition is mild, and energy consumption is relatively low, so it has been widely studied and applied. The properties of PS activated by different transition metal ions have been investigated over the past decades. Transition metal ions mainly transfer a single electron to realize the activation function. The reaction process is shown in Equation (1).

$$S_2O_8^{2-} + \mathrm{Mn}^{n+} \rightarrow SO_4{\cdot}^- + SO_4^{2-} + \mathrm{Mn}^{(n+1)+} \tag{1}$$

Common transition metal ions used to activate PS include Fe^{2+}, Ag^{+}, Co^{2+}, Mn^{2+}, and Cu^{2+}. Different metal ions show different activation properties under the same reaction conditions. The optimal combination of metal ions and oxidants depends on the target pollutant and reaction conditions (Wacławek *et al.* 2017). It seems that Ag^{+} is more effective than other ions in activating PDS to degrade organic pollutants (Gong & Lin 2011; Parenky *et al.* 2020), whereas Co^{2+} is more suitable for activating PMS (Anipsitakis & Dionysiou 2004). However, rare metals such as Ag and Co can easily cause secondary pollution to human body and environment, which greatly limits their practical application in groundwater treatment. By contrast, iron is considered as one of the most feasible PS activators because of its non-toxicity, environmentally friendliness and low-cost (Rastogi *et al.* 2009; Bae *et al.* 2018).

Commonly used iron-based materials activating PS to degrade the organics include Fe^0, Fe^{2+}, Fe^{3+}, and iron minerals (Fe_2O_3, Fe_3O_4, and $Fe_{1-x}S$), and the main activated species is attributed to the generation of Fe^{2+}. The activation of PS by Fe^{2+} is mainly achieved through donating one electron to PS, leading to the break of O–O bonds in the PS molecular structure, and the formation of $SO_4{\cdot}^-$ and SO_4^{2-} (Equation (2)). Interestingly, researchers found that Fe^{3+} could also react with S_2O8^{2-} to form Fe^{2+}, as shown in Equation (3), therefore Fe^{2+} and Fe^{3+} can transform cyclically in the Fe^{2+}/PS system.

$$Fe^{2+} + S_2O8^{2-} \rightarrow Fe^{3+} + SO_4^{2-} + SO_4{\cdot}^- \tag{2}$$

$$Fe^{3+} + S_2O8^{2-} \rightarrow Fe^{2+} + S_2O8{\cdot}^- \tag{3}$$

Previous studies argued that the reaction between the transition metals and PS could produce $\cdot OH$ as the sole oxidant species, but recent studies have shown that the reaction also generates high-valence metals (Huang *et al.* 2016; Jin *et al.* 2020), which can also participate in the degradation of organic pollutants. It has been reported that transition metals, such as Fe, Co, Mn, and Cr, can form reactive high-valence metals during the PS activation process (Wang *et al.* 2018; Zong *et al.* 2020). With high reactivity, the generated high-valence metals can selectively degrade some refractory organic pollutants, and usually they will be converted to the original valence state after the reaction, thus continuous reaction can

be maintained (Wang *et al.* 2018, 2019b). It has been found that Fe(IV) is generated in the system when Fe(II) is used to activate PDS (Dong *et al.* 2020). Fe(IV) can react with organic matter, then it is converted to Fe(II), so Fe(II) is hardly consumed during the reaction process. PS acts as an electron acceptor to provide oxygen atoms during the formation of high-valence metals (Zong *et al.* 2020). The action mechanism of the high-valence metal is shown in Equations (4) and (5). (M^{V+} refers to metal ions with higher valence states than M^{n+}.)

$$M^{n+} + HSO_5^- \rightarrow M^{V+} + OH^- + SO_4\cdot^- \quad (4)$$

$$M^{n+} + S_2O_8^{2-} \rightarrow M^{V+} + SO_4\cdot^- + SO_4^{2-} \quad (5)$$

Although Fe^{2+} can be used alone to effectively activate PS, there are still some issues that need to be addressed. Firstly, acidic conditions are required for this process (Boczkaj & Fernandes 2017), and Fe^{2+} reacts very quickly with PS, usually within a few minutes. Secondly, Fe^{2+} is highly reductive, it will participate in a variety of redox reactions during the PS activation process, so it is easily oxidized to Fe^{3+}, losing the ability to activate PS. To overcome these deficiencies, ZVI is used as a source of Fe^{2+} to activate PS for degradation of contaminants. The feasibility of degrading CHCs by activated PS using ZVI as the Fe^{2+} source has been demonstrated (Rajajayavel & Ghoshal 2015; Han & Yan 2016). Fe^0 is more effective than Fe^{2+} in activating PS for mineralization of contaminants (Oh *et al.* 2009; Kusic *et al.* 2011; Barzegar *et al.* 2018). On the one hand, it releases Fe^{2+} slowly in case of excessive presence of Fe^{2+} in the system (Fang *et al.* 2013a). On the other hand, it is superior in terms of subsurface migration (Kim *et al.* 2018; Wu *et al.* 2019). It is worth noting that the ZVI particle size affects the release rate of Fe^{2+} (Rodriguez *et al.* 2014). Smaller particles of ZVI usually needs less time to release Fe^{2+}, the higher PS activation efficiency can be achieved.

3. ACTIVATION OF PS BY ZVI-BASED MATERIALS

3.1. ZVI/nZVI

Both ZVI and nanometer ZVI (nZVI) can serve as stable sources of Fe^{2+}. Although they have the same valence state, their surface structures are different. nZVI has a larger specific surface area than ZVI, which gives it stronger adsorbability, reactivity, and subsurface mobility (Lefevre *et al.* 2016). The catalytic performance of nZVI, ZVI, and Fe^{2+} for PS degradation of TCE has been studied (Al-Shamsi & Thomson 2013). The results showed that TCE degradation rate was the fastest in the nZVI/PS system, its degradation rate in the first 3 min was 21 times higher than that in the ZVI/PS system.

It is recognized that Fe^{2+} is the main activated species in Fe/PS system, thus it is crucial to analyze its source. Fe^{2+} can be produced by nZVI in the PS activation system through a variety of reaction pathways. First, Fe^0 can lose an electron and decompose into Fe^{2+} as described in Equation (6). Second, in both aerobic and anaerobic conditions, Fe^0 can be corroded to produce Fe^{2+} (Equations (7) and (8)). For a long time, researchers believed that Fe^{2+} was the main or even sole iron-based activation species in PS system (Kim *et al.* 2018). Nevertheless, other researchers proposed that Fe^0 could directly react with PS to generate Fe^{2+} as described in Equation (9) (Duan *et al.* 2015; Rayaroth *et al.* 2017). Moreover, Fe^{3+} could also react with Fe^0 to form Fe^{2+} (Equation (10)), promoting the recycling of Fe^{2+}.

$$Fe^0 \rightarrow Fe^{2+} + 2e^- \quad (6)$$

$$2Fe^0 + O_2 + 2H_2O \rightarrow 2Fe^{2+} + 4OH^- \quad (7)$$

$$Fe^0 + 2H_2O \rightarrow Fe^{2+} + 2OH^- + H_2 \quad (8)$$

$$Fe^0 + S_2O_8^{2-} \rightarrow Fe^{2+} + 2SO_4^{2-} \quad (9)$$

$$Fe^0 + 2Fe^{3+} \rightarrow 3Fe^{2+} \quad (10)$$

In the above reactions of the nZVI/PS system, Fe^{2+} mainly comes from the electron transfer of Fe^0 (Liang & Lai 2008). It should be noted that when Fe^{2+} is excessive in the system, it is more likely to be consumed by $SO_4\cdot^-$ rather than to activate PS (Equation (11); Hou *et al.* 2021). Thus, excess Fe^{2+} can limit the oxidation capability of the system (Liang *et al.* 2004), leading

to the simultaneous removal of $SO_4\cdot^-$ and Fe^{2+} from the system, and a lower pollutant removal rate.

$$Fe^{2+} + SO_4\cdot^- \rightarrow Fe^{3+} + SO_4^{2-} \quad (11)$$

Also, some researchers proposed that Fe^{2+} was not the sole activator in the nZVI/PS system, they believed that Fe^0 could activate PS directly to produce oxidizing radicals (Oh *et al.* 2010). Oh *et al.* (2010) indicated that the optimal molar ratio of PS to nZVI was 1 during the degradation of 2,4-dinitrotoluene (DNT), in which no $SO_4\cdot^-$ was generated theoretically via reaction Equation (9), and more PS was required to produce $SO_4\cdot^-$, which was bound to increase the molar ratio of PS to nZVI to above 1. Thus, a separate mechanism was proposed that electrons could directly transfer from the nZVI surface to PS. However, the optimal molar ratio of PS to nZVI should be related to the target pollutant and not fixed (Hou *et al.* 2021). Therefore, the theoretical view that electrons transfer directly from nZVI to PS is unreliable.

The concentrations of PS and Fe^{2+} in solution are crucial parameters for the formation of $SO_4\cdot^-$, and the molar ratio of Fe^{2+} to PS also determines the yield of $SO_4\cdot^-$. Generally, the CHCs removal reaction is divided into two stages: in the initial stage of the reaction, the CHCs removal rate increases with the increase of Fe^{2+} or PS concentration. After the initial phase, the removal rate will decrease even if the concentration of Fe^{2+} or PS continues to increase (Gu *et al.* 2015). This suggests that an appropriate molar ratio of Fe^{2+} to PS, rather than a higher concentration of Fe^{2+} or PS, can obtain a better CHCs removal rate.

It has been mentioned above that transition metal ions can be oxidized to higher valence states during activation of PS (Wang *et al.* 2018). The formation of hypervalent metals is caused by the oxidation of transition metals by PS, resulting in formation of two oxidizing species – free radicals and hypervalent metals, both of which can degrade organic pollutants. However, the ability of high-valence metals removing organic pollutants is not absolute. The current consensus is that the reaction mechanism of hypervalent metals can transform organic pollutants, but cannot further completely mineralize them. Recent studies have confirmed that ferryl iron (Fe(IV)) is produced during degradation of sulfone organics in the nZVI/PS system. Fe(IV) converts the target pollutants to other forms without mineralizing the contaminants (Wang *et al.* 2020).

Although nZVI, as a heterogeneous PS activator, can effectively slow the release of Fe^{2+} and promote the generation of $SO_4\cdot^-$, the degradation of pollutants almost stops after a period of reaction, and the remaining PS in the system cannot be decomposed for further oxidation. The reason for this phenomenon is that iron oxides such as Fe_2O_3, Fe_3O_4, and FeOOH are generated on the surface of nZVI during the activation of PS (Li *et al.* 2014a). As shown in Figure 1, the iron oxide complexes and FeOOH cover the core of nZVI, which reduces the number of active sites for nZVI catalytic activation of PS, thus greatly inhibiting the persistence of nZVI activation. Al-Shamsi & Thomson (2013) used the nZVI activating PS system to treat TCE, and found that the initial degradation rate was very fast, but decreased to the order of magnitude of unactivated

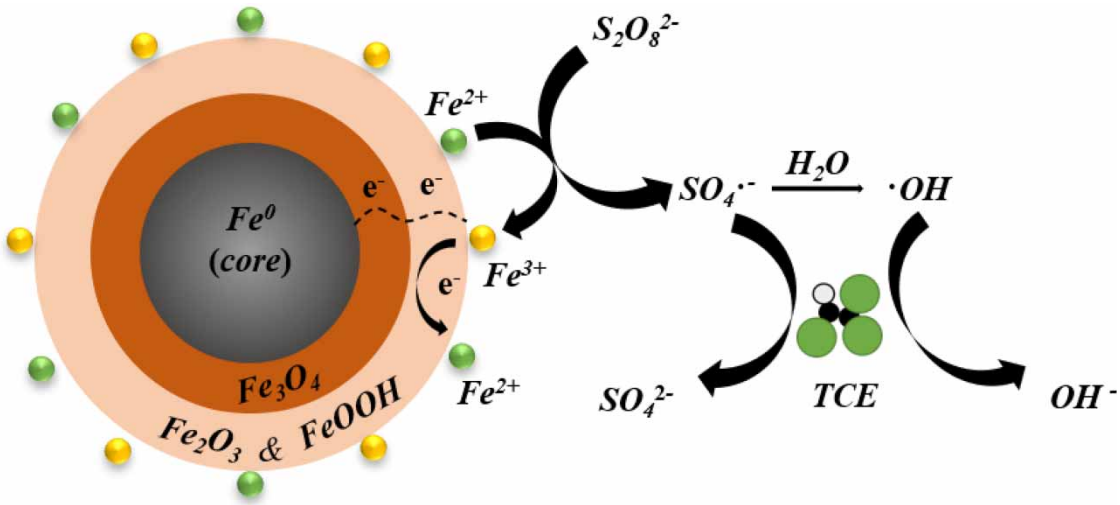

Figure 1 | Mechanism of nZVI activating PS to degrade TCE.

PS systems after about 50 min, which might be attributed to the generation of iron oxide complexes, leading to passivation of the nZVI surface.

Besides, nZVI particles tend to aggregate due to strong interparticle attraction and inherent magnetic interaction (Li *et al.* 2011; Rayaroth *et al.* 2017), which usually results in low mobility and weak reactivity. In addition, nZVI is susceptible to be oxidized in aqueous solution, resulting in its stability and utilizability being reduced (Fan *et al.* 2016a; Bae *et al.* 2018). These defects limit its application in soil and groundwater remediation.

3.2. Modified nZVI

Given the above drawbacks of nZVI during the PS activation process, a novel material with good slow-release Fe^{2+} function, strong sustained performance, and suitability for migration in soil voids has become a focus of research. The aim of modified nZVI is to improve the PS activation ability and to enhance its mobility and stability in groundwater. Up to now, a variety of modified nZVI materials have been developed. The four main types of modification methods for nZVI that have been widely studied are supported nZVI, bimetallic modification, sulfide-modified nZVI, and surface-coated nZVI.

3.2.1. Supported nZVI

Heterogeneous support refers to the combination of nZVI with a solid carrier such as silica gel, carbon, or polymeric resin. In order to effectively hinder the aggregation of nZVI particles and enhance the reactivity, the above materials can be used as a supporter, so that nZVI particles can be evenly and stably dispersed on the surface of the material to form supported nZVI (Yu *et al.* 2019). With large specific surface area, large pore volume, low cost, and wide sources, carbon has become the most widely used supported material (Liu *et al.* 2016b; Fan *et al.* 2019). The carbon-supported nZVI composite can improve the adsorption capacity of the catalyst and it has been shown to be effective in activating PS to degrade contaminants (Wang *et al.* 2015). Commonly used carbon-based materials include activated carbon (AC), biochar (BC), reduced graphene oxide (rGO), and carbon nanotubes (CNTs) (Huang *et al.* 2014b; Wu *et al.* 2018a).

Carbon-based adsorbent, with high specific surface area and porosity, owns extremely strong adsorption capacity (Wei *et al.* 2018). The adsorption of the carrier can increase the contact chance between nZVI and pollutants so as to accelerate the reaction rate (Fan *et al.* 2019). When nZVI is uniformly supported on the surface of carbon-based materials, the aggregation phenomenon between particles can be eliminated (Mandal *et al.* 2020). Meanwhile, the mobility of nZVI is significantly enhanced, thus the reactivity can be improved (Yang *et al.* 2018). The degradation effect of nZVI/BC/PS system on TCE has been studied (Yan *et al.* 2015). In the absence of activator, PS itself cannot effectively degrade TCE. When nZVI was used as an activator, the degradation rate of TCE was significantly improved. By contrast, nZVI/BC composite catalyst was selected to activate PS for removing TCE, the degradation rate was much higher than that of pure nZVI (Shan *et al.* 2021a).

As for the reactive species, different from the nZVI/PS system that $\cdot OH$ and $SO_4\cdot^-$ are absolutely dominant, other active groups (such as oxygen-rich functional groups) are also found to be involved in degradation of organic pollutants in the BC-nZVI/PS system. Ravikumar *et al.* (2018) found that oxygen-rich functional groups (such as –OH and –COOH) on the surface of BC could rapidly adsorb organic pollutants and degrade them to some extent. In addition, these groups could also directly catalyze PS to produce $SO_4\cdot^-$ for degradation of refractory organic compounds (Tan *et al.* 2016; Xu *et al.* 2018; Equations (12) and (13).

$$-COOH + S_2O8^{2-} \rightarrow -COO\cdot + HSO_4^- + SO_4\cdot^- \quad (12)$$

$$-OH + S_2O8^{2-} \rightarrow -O\cdot + HSO_4^- + SO_4\cdot^- \quad (13)$$

rGO also provides rich adsorption sites for nZVI immobilization due to its unique two-dimensional layered structure and large specific surface area (Hao *et al.* 2018). The activation mechanism of PS by rGO-nZVI is similar to that by BC-nZVI. In addition to supporting nZVI, oxygen-rich functional groups such as –COOH and –OH on the surface of rGO also catalyze PS to release $\cdot OH$ and $SO_4\cdot^-$ (Wu *et al.* 2018a). In addition, $O_2\cdot^-$ is also found in the rGO- nZVI system as one of the active free radicals (Ahmad *et al.* 2015), and $SO_4\cdot^-$ tends to be produced under acidic conditions, while $O_2\cdot^-$ prefers alkaline conditions.

It is worth noting that carbon materials are easily deactivated by oxidation of free radicals, and the small molecular organic matter produced in the reaction process tends to block the internal pores of the carbon, and mask the active sites, thus reducing the removal capacity of pollutants (Wu *et al.* 2018b; Wang *et al.* 2019a).

3.2.2. Sulfide-modified nZVI

Sulfide-modified nZVI (S-nZVI) is the chemical modification of nZVI by adding sulfide agent to form iron pyrite on the surface of nZVI particles. Research on sulfidation of nZVI has received increasing attention recently due to its ability to improve the reactivity of nZVI. S-nZVI has lower hydrophilicity and less magnetism than nZVI (Xu *et al.* 2019a; Mangayayam *et al.* 2020; Li *et al.* 2021a), which is mainly attributed to the formation of an iron sulfide (FeS_x) protective shell on the surface of nZVI. FeS_x can increase the surface roughness and specific surface area of the particles, which inhibits nZVI aggregation, facilitates the adsorption of pollutants, and improves the reactivity (Cao *et al.* 2017; Song *et al.* 2017). FeS_x on the surface of nZVI also prevents the corrosion reaction between nZVI and H_2O, and inhibits hydrogen precipitation (Han & Yan 2016), driving more nZVI to participate in the activation reaction.

Two main types of iron sulfide are formed in the nZVI sulfidation process, namely FeS and FeS_2. Both of them have been proven to be effective for PS activation (Fan *et al.* 2018; Lian *et al.* 2019). However, FeS minerals are generally considered to be more hydrophobic and more conductive than FeS_2 (Zhang *et al.* 2016; Sun *et al.* 2018). Therefore, S-nZVI with a FeS shell is selected for most laboratory research and engineering applications.

Meanwhile, sulfidation can also enhance the conductivity of nZVI. Delocalized electrons in the FeS interlayer can be used as an electronic conductor, promoting transfer of electrons from nZVI to pollutants, and improving the degradation rate (Kim *et al.* 2011; Li *et al.* 2016). Kim *et al.* (2011) studied the influence of sulfidation on the surface potential and conductivity of nZVI and found that the electronic mobility was significantly enhanced on the surface of S-nZVI.

Although the formation of FeS_x on the surface of nZVI increases the distance between particles and inhibits the aggregation of nZVI, there is no significant difference in the aggregation behavior between S-nZVI and nZVI when divalent cations exist in the system (Song *et al.* 2017). This is mainly attributed to that the aggregation between S-nZVI particles is affected by the inhibition of electrostatic repulsion, while divalent cations can shield the electrostatic charge on the surface of iron nanoparticles (Adeleye *et al.* 2013). Thus, the aggregation is not eliminated.

Considering that S-nZVI possess more advantages than nZVI, it can be inferred that S-ZVI has a better effect in activating PS to degrade pollutants. One difference between the two structures is that FeS is generated on the surface of S-nZVI, whereas FeOOH and Fe_xO_y are formed on the nZVI particle surface. Mangayayam *et al.* (2019) showed that some $Fe(OH)_2$ structures are formed on the surface of S-nZVI, but FeS is still the main structure of the S-nZVI shell. The FeS deposited on the S-nZVI surface prevents the passivation of the nZVI surface because of the absence of FeOOH and Fe_xO_y, and facilitates more electron transfer from the iron core to the surface, leading to the continuous formation of surface-bound iron available for PS activation (Equation (14)); Dong *et al.* 2019).

$$Fe^0 + Fe - S - Fe^{3+} \rightarrow Fe - S - Fe^{2+} \tag{14}$$

In recent years, S-nZVI has been successfully applied to activate PS to remove CHCs. Recent research confirmed that it was difficult to degrade TCE using PS or S-nZVI alone. The activation of PS by nZVI could reduce the concentration of TCE to a certain extent, and the removal rate of TCE by using S-nZVI/PS was higher than that of nZVI/PS at various pH conditions (Dong *et al.* 2019). Thus, S-nZVI was superior to nZVI in activating PS to degrade TCE. However, the dechlorination efficiency of the two did not show a significant difference. The dechlorination efficiency of TCE in acidic, neutral, and alkaline conditions was 45.83, 38.10, and 35.28% in the S-nZVI/PS system, and that was 41.71, 35.90, and 33.49% in the nZVI/PS system, respectively. This result indicated that only a portion of the TCE was completely degraded in the S-nZVI/PS system.

It should be noted that the activation effect is not proportional to the sulfide content. The reactivity of S-nZVI is affected by many factors, particularly the S/Fe molar ratio (Li *et al.* 2017). With the molar ratio increasing, more iron sulfide is generated on the surface of the S-nZVI, improving its conductivity and facilitating removal of organics. However, hollow structures will be formed as the molar ratio is excessive, reducing the reactivity of the S-nZVI (Xu *et al.* 2019b). Besides, a high molar ratio will lead to FeS_2, with lower reactivity, accumulated on the surface (Xie & Cwiertny 2010; Nunez *et al.* 2016), which decreases the dosage of nZVI and the surface area of composite materials, and further reduces the pollutant removal ability (Song *et al.* 2017; Dong *et al.* 2018).

3.2.3. Bimetallic materials

Heterogeneous materials based on metal catalysts are widely used for PS oxidation due to the easy recovery and wide sources. In recent years, metal PS catalysts have been developed from single metal form to bimetal or even polymetallic forms.

Bimetallic nanoparticles formed by adding less reactive metals to nZVI can increase the reactivity of the particles and provide good protection against passivation (Yan *et al.* 2013). nZVI composites with other metals are one of the most widely studied bimetal systems because of their high reactivity and large specific surface area, and they have been applied in treatment of halogenated organically polluted wastewater (Su *et al.* 2016; Zhu *et al.* 2016). The catalytic activity of metal catalysts to PS is enhanced by their synergistic effect, such as electron transfer and their ilka catalytic effect on PS. Metals commonly doped to nZVI to form bimetallic system include Co, Cu, Ni, Pt, Ag, and Pd (Li *et al.* 2021b). Ag and Ni are toxic, Pt and Pd are rare and expensive, which restricts their environmental applications. Cu is relatively inexpensive and less toxic than other several precious metals, therefore it has been increasingly combined with nZVI. Researchers prefer to choose Cu doped onto nZVI to activate PS for removing organic pollutants.

In the nZVI–Cu/PS system, PS is firstly activated by Fe^{2+} to produce some oxidation radicals. It is know that an oxide layer is easy to be formed on pure nZVI surface, which blocks a large number of active sites on the surface and inhibits electron transfer, reducing the removal efficiency of pollutants. The presence of Cu alleviates this problem effectively. The reactivity of organic pollutants in the Fe/Cu/PS system has been shown to be much superior than that in the Fe/PS system (Xiong *et al.* 2015). Based on the mechanism of nZVI activating PS, Cu^0 is dissolved into Cu^{2+} in the Fe/Cu/PS system, and then Cu^{2+} activates PS to produce Cu^{3+}, $SO_4\cdot^-$, and SO_4^{2-} (Equations (15) and (16); Liang *et al.* 2013; Popescu *et al.* 2015). However, the Cu^{3+} is extremely unstable and easily reduced by the abundant Fe^0 in the solution (Equation (17)). Also, Cu^+ appears in the system and participates in the reaction. This phenomenon is particularly significant under acidic conditions. Zhou *et al.* (2018) found that almost all Cu^0 dissolves into the Cu^+ in an acidic solution, which in turn activates PS to produce free radicals, as shown in Equations (18) and (19).

$$Cu^0 + S_2O_8^{2-} \rightarrow Cu^{2+} + 2SO_4^{2-} \tag{15}$$

$$Cu^{2+} + S_2O_8^{2-} \rightarrow Cu^{3+} + SO_4\cdot^- + SO_4^{2-} \tag{16}$$

$$2Cu^{3+} + Fe^0 \rightarrow 2Cu^{2+} + Fe^{2+} \tag{17}$$

$$2Cu^0 + 2H^+ \rightarrow 2Cu^+ + H_2 \tag{18}$$

$$Cu^+ + S_2O_8^{2-} \rightarrow Cu^{2+} + SO_4\cdot^- + SO_4^{2-} \tag{19}$$

Besides, acidic conditions can accelerate corrosion of nZVI–Cu, releasing more Fe^{2+} and producing extra $SO_4\cdot^-$ (Lai *et al.* 2013; Hussain *et al.* 2017), thus achieving higher removal rate of pollutants than that in neutral or alkaline solutions. The synthesized bimetallic particles form galvanic cells on nZVI surface, promoting electron transfer and accelerating the reaction degree (Shi *et al.* 2016; Zeng *et al.* 2017). However, studies have confirmed that excessive Cu might inhibit nZVI corrosion, and the amount of doped copper required to achieve the highest removal rate differs for different pollutants (Qu *et al.* 2020).

In order to evaluate the CHCs degradation ability of bimetallic materials activating PS, relevant studies were also conducted. Polyvinylpyrrolidone functionalized Fe/Cu bimetallic nanoparticles (PVP-nZVI/Cu) were synthesized and used to activate PS for degradation of TCE (Idrees *et al.* 2021). It was found that about 5.3 and 7.1% of TCE was lost by PVP-nZVI/Cu and PS alone, respectively. PVP-nZVI activated PS obtained 68.8% of TCE removal rate. By contrast, PVP-nZVI/Cu nanoparticles could almost completely remove TCE.

Bimetallic-modified nZVI materials improve the reactivity and pollutant removal rate to some extent. However, up to now they are mostly used in remediation of heavy metal contaminated soil and groundwater in practical applications (Zhu *et al.* 2017, 2018b, 2018c), but rarely in combination with PS for degradation of CHCs.

3.2.4. Surface-coated nZVI

Due to the van der Waals force and magnetic properties of iron, as well as the surface energy of nanometer materials, nZVI particles tend to agglomerate, affecting their migration and reactivity in soil and groundwater (Jiemvarangkul *et al.* 2011). Therefore, improving the dispersion of nZVI has become a research hotspot in recent years.

The purpose of nZVI surface modification is to increase its dispersion and liquidity in water medium, and the ideal modifier is characterized by strong adherence to the particle surface, strong stability, and no secondary pollution. The surface modification mechanism mainly changes the surface charge distribution of nZVI through adsorption of the modifier, and prevents electrostatic attraction and aggregation of nZVI by means of electrostatic stability, steric hindrance, or the combination of the two (Tesh & Scott 2014; Zhao *et al.* 2016). One method to maintain the nZVI particles in stable state is to increase the electrostatic repulsion between them. Several studies have demonstrated that certain polymeric materials can stabilize nanoparticles in aqueous solutions, including polyacrylic acid (PAA), polyaspartic acid (PAP), Tween 80, and biopolymers such as soy protein, starch, and carboxymethyl cellulose (CMC) (Liu *et al.* 2016a; Saha *et al.* 2019; Li *et al.* 2020). Different types of surface modifiers have been used to coat nZVI particles, ranging from long-chain polyelectrolytes such as polyethylene vinyl pyrrolidone (PVP) and CMC, to short-chain surfactants such as rhamnol (RL) (Bhattacharjee *et al.* 2016). High-concentration nZVI aqueous dispersion has been obtained after modification by Tween 80 (Soukupova *et al.* 2015). Compared with unstabilized nZVI, nZVI modified by Tween 80 has been shown strong oxidation resistance, time stability, as well as high reactivity to target pollutants. It is possible that the surface layer formed by Tween 80 on the particles plays a key role. Biosurfactants such as rhamnolipid have also been shown to be excellent surface modifiers, significantly reducing accumulation of nZVI and improving its transportation (Liang *et al.* 2014).

CMC is currently one of the most widely used polysaccharide derivatives for nZVI modification. Complexation between the carboxylic acid base group and iron ions, as well as the intermolecular hydrogen bonds between CMC and the iron particle surface, are considered to be the main mechanisms of stabilization. Fatisson *et al.* (2010) synthesized coated nZVI by CMC, and studied the effect of organic matter in natural water on the aggregation and surface charge of nanoparticles before and after coating. The results showed that CMC was bonded to the surface of the nanoparticles by covalent bonds, which effectively inhibited their aggregation in solution. The study also found that electrostatic repulsion was the main reason why CMC inhibited aggregation of nZVI particles. Meanwhile, CMC surface modification could also reduce the average size of nZVI nanoparticles and improve their specific surface area (Eljamal *et al.* 2020), which was conducive to the removal of pollutants. Dong *et al.* (2016) found that CMC-coated nZVI not only showed good dispersity and stability, but also had low toxicity to cells, alleviating the long-standing concerns about nZVI practical application.

Although surface modification has been used for field testing, the main disadvantage is that coating can occupy the reactive sites of the nZVI, which affects its ability to react with contaminants and decreases the pollutant removal efficiency. Meanwhile, there is still little research to date on the oxidation degradation of CHCs by CMC-modified nZVI activating PS, most of which focuses on the reduction effect of CMC-nZVI on CHCs. In order to facilitate the comparison of the advantages and disadvantages of the four modification methods, the above contents are simply summarized (as shown in Table 1).

Table 1 | Comparison of different modification methods of nZVI

Modification methods	Structural difference	Advantages	Disadvantages
Supported nZVI	Oxygen-rich functional groups (such as –OH and –COOH) is formed on catalyst surface	Improving the specific surface area, adsorbability, reactivity, and mobility	Carbon materials are easily deactivated by oxidation of free radicals
Sulfidation	An iron sulfide (FeS_x) protective shell is formed	Inhibiting nZVI aggregation, improving the oxidation resistance, conductivity, adsorbability of pollutants, and reactivity	Hollow structures will be formed as the S/Fe molar ratio is excessive, reducing the reactivity of the S-nZVI
Bimetallic materials	Form galvanic cells, promoting electron transfer	Improving oxidation resistance, time stability, as well as reactivity	Rare metals are expensive, easy to cause environmental pollution, practical applications are few
Surface-coated nZVI	Form a complete micelle and a protective layer on the surface of ZVI	Enhancing oxidation resistance, particle stability, subsurface mobility; reducing aggregation	Coating can occupy the reactive sites of the nZVI, affecting its ability to react with contaminants and decreasing the pollutant removal efficiency

3.3. The dominant active species

There has been a long debate about the dominant role of oxidizing species in the degradation of organic pollutants in the nZVI/PS system. Generally, $SO_4\cdot^-$ is considered to be the major free radical in the system (Al-Shamsi & Thomson 2013; Ayoub & Ghauch 2014). However, later studies confirmed that $\cdot OH$ also participated in degradation of pollutants, and its contribution was sometimes more significant than that of $SO_4\cdot^-$ (Yuan *et al.* 2014; Rayaroth *et al.* 2017; Huang *et al.* 2019). The following three pathways may be responsible for $\cdot OH$ formation. Firstly, the hydrolysis of PS and the continuous Fenton reaction may lead to $\cdot OH$ generation through Equations (20) and (21). Secondly, the reaction of nZVI with O_2 can also produce $\cdot OH$, $O^{2-}\cdot$, and $SO_4\cdot^-$ in solution (Equations (22)–(25)). In addition, $SO_4\cdot^-$ can react with H_2O to produce $\cdot OH$ (Equation (26)).

$$S_2O_8^{2-} + 2H_2O \rightarrow 2HSO_4^- + H_2O_2 \tag{20}$$

$$Fe^{2+} + H_2O_2 \rightarrow Fe^{3+} + \cdot OH + OH^- \tag{21}$$

$$Fe^0 + O_2 + 2H^+ \rightarrow Fe^{2+} + H_2O_2 \tag{22}$$

$$Fe^{2+} + H_2O_2 \rightarrow Fe^{3+} + \cdot OH + OH^- \tag{23}$$

$$Fe^{2+} + O_2 \rightarrow Fe^{3+} + O_2\cdot^- \tag{24}$$

$$S_2O_8^{2-} + O_2\cdot^- \rightarrow SO_4^2 - + SO_4\cdot^- + O_2 \tag{25}$$

$$SO_4\cdot^- + H_2O \rightarrow \cdot OH + SO_4^{2-} + H^+ \tag{26}$$

In order to more comprehensively understand the degradation mechanism of CHCs by the nZVI/PS system, researchers conducted a number of exploratory experiments, and the debate about which of the two is dominant has not been settled.

Theoretically, the produced $SO_4\cdot^-$ by the reaction between Fe^{2+} and PS can directly oxidize the target pollutants, $SO_4\cdot^-$ is the dominant active species in the system. Table 2 shows the recent research literatures on degradation of CHCs by iron-based materials activating PS, most studies show that $SO_4\cdot^-$ is dominant only under acidic conditions, and the contribution of $\cdot OH$ seems to be more prominent in neutral or alkaline environments. The reasons for this phenomenon can be explained by Figure 2. Under acid conditions, the modified nZVI/PS system will produce more dissolved Fe^{2+}, which can promote the decomposition of PS to produce more $SO_4\cdot^-$. On the contrary, under neutral and alkaline conditions, the amount of released Fe^{2+} will decrease and more iron will precipitate in the form of ferric hydroxide and ferrous hydroxide, further reducing the effect of PS activation (Yuan *et al.* 2015). Besides, $SO_4\cdot^-$ is more likely to react with H_2O or OH^- to produce $\cdot OH$ under neutral and alkaline conditions (Equations (26) and (27)), rather than to degrade pollutants directly, so $\cdot OH$ plays a major role. Meanwhile, H^+ is released during the process. It is a safe guess that most $\cdot OH$ in the system comes from this process, because the pH of the solution has been found to decrease significantly after the reaction, especially under neutral and alkaline conditions (Huang *et al.* 2019; Shan *et al.* 2021b; Sun *et al.* 2021; Xu *et al.* 2021a). In addition, $\cdot OH$ can be produced by the oxidation of water as described in Equation (28). Thus even though $SO_4\cdot^-$ has a stronger redox potential and a longer half-life, its utilization efficiency is far lower than $\cdot OH$ under neutral and alkaline conditions.

$$SO_4\cdot^- + OH^- \rightarrow SO_4^{2-} + \cdot OH \tag{27}$$

$$Fe^0 + 2S_2O_8^{2-} + 2H_2O \rightarrow Fe^{2+} + 2\cdot OH + 4SO_4^{2-} + 2H^+ \tag{28}$$

Recent studies have found that in addition to $\cdot OH$ and $SO_4\cdot^-$, other super-active intermediates (such as $HO_2\cdot$ and $O_2\cdot^-$) are also involved in the reaction during the generation of free radicals by PS activation (Fang *et al.* 2021; Idrees *et al.* 2021). Under certain conditions, H_2O_2 produced by $\cdot OH$ self-quenching reacts with $\cdot OH$ and $SO_4\cdot^-$ to form $HO_2\cdot$, which can be further decomposed to form $O_2\cdot^-$ (redox potential = −2.4 V) (Equations (29)–(32)). $O_2\cdot^-$ effectively reduces and degrades volatile CHC pollutants that are difficult to oxidize. Free radical scavenging experiments verified that $O_2\cdot^-$ is one of the

Table 2 | Summary of degradation of CHCs by iron-based materials activated PS

Oxidation system	Contaminant	Reaction pH	Reaction conditions	Maximum removal rate	Reactive oxygen species	References
S-nZVI/PS	TCE	2.32–9.58	$[S\text{-nZVI}]_0 = [PS]_0 = 5$ mM, $[TCE]_0 = 1$ mM	90.7%	$\cdot OH$ and $SO_4\cdot^-$ contribute almost equally under acidic condition, while the dominance of $\cdot OH$ was more obvious under neutral and alkaline conditions	Dong *et al.* (2019)
Fe(II)/S-nZVI/PS	TCE	3.0–9.0	$[PS]_0 = 0.60$ mM, $[Fe(II)]_0 = 0.30$ mM, $[S\text{-nZVI}]_0 = 0.30$ mM, $[TCE]_0 = 0.15$ mM	99.6%	Both $\cdot OH$ and $SO_4\cdot^-$ were responsible for the degradation, and $\cdot OH$ was greater significance than $SO_4\cdot^-$ (ignoring initial pH)	Zhou *et al.* (2021)
Zeolite-supported nZVI/PS	TCE	7.0	$[TCE]_0 = 0.15$ mM, $[PS]_0 = 1.5$ mM, $[Z\text{-nZVI}]_0 = 168$ mg/L	98.8%	$\cdot OH$ and $SO_4\cdot^-$, $\cdot OH$ was relatively more dominant	Huang *et al.* (2019)
PS/Fe(II)/citric acid	TCE	3.0	Molar ratio of PS/Fe(II)/CA/TCE is 30/4/4/1	97.5%	$\cdot OH$ and $SO_4\cdot^-$, $SO_4\cdot^-$ was relatively more dominant	Sun *et al.* (2021)
PS/Fe(II)/hydroxylamine	TCE	Unadjusted	Molar ratio of PS/Fe(II)/HA/TCE is 15:2:10:1	97.9%	$SO_4\cdot^-$,$\cdot OH$ and $O_2\cdot^-$, $\cdot OH$ was dominant	Wu *et al.* (2015)
Attapulgite-supported nZVI/PS	TCE	3.50	$[TCE]_0 = 5$ mg/L, $[PS]_0 = 1.0$ mM, $[AT\text{-nZVI}]_0 = 0.4$ g/L	90.4%	$\cdot OH$ and $SO_4\cdot^-$, $\cdot OH$ was dominant	Zhang *et al.* (2022)
Biochar-supported nZVI–Ni/PS	TCE	3.0	$[nZVI\text{-i@BC}]_0 = 0.25$ g/L, $[PS]_0 = 4.0$ mM, $[TCE]_0 = 0.15$ mM	98.8%	Both $\cdot OH$ and $SO_4\cdot^-$ were dominant role in acidic environment	Shan *et al.* (2021a)
PS/Fe(II)/nZVI/PS with TW-80	TCE	5.55	$[PS]_0 = 1.2$ mM, $[Fe(II)]_0 = 0.6$ mM, $[nZVI]_0 = 0.6$ mM, $[TCE]_0 = 0.15$ mM, $[TW\text{-}80]_0 = 13$ mg/L	99.5%	$\cdot OH$ and $SO_4\cdot^-$ contributed a major part while $O_2\cdot^-$had small contribution	Xu *et al.* (2021a)
S-FeNi@BC/PS	TCE	3.20	$[S\text{-FeNi@BC}]_0 = 0.4$ g/L, $[PS]_0 = 1.5$ mM, $[TCE]_0 = 0.15$ mM	98.4%	$SO_4\cdot^-$,$\cdot OH$, $O_2\cdot^-$ and $^1O_2$, $SO_4\cdot^-$ had greater contribution than $\cdot OH$	Shan *et al.* (2021b)
nFe_3O_4/rGO/PS	TCE	3.0–11.0	$[nFe_3O_4/rGO]_0 = 6.94$ g/L, $[PS]_0 = 3.0$ mM, $[TCE]_0 = 0.15$ mM	98.6%	Under acidic and basic conditions, the dominant radical was $SO_4\cdot^-$ and $\cdot OH$, respectively	Yan *et al.* (2016)
ZVI/PS	TCA	6.0	$[PS]_0 = 9.0$ mM, $[TCA]_0 = 0.15$ mM, $[ZVI]_0 = 0.05$ g	97%	Both $\cdot OH$ and $SO_4\cdot^-$ were dominant role	Gu *et al.* (2015)
FeS_2/PMS	TCA	2.0–12.0	$[TCA]_0 = 0.15$ mM, $[PMS]_0 = 5$ mM, $[FeS_2]_0 = 0.8$ g/L	90%	$SO_4\cdot^-$,$\cdot OH$, $O_2\cdot^-$ and $^1O_2$, $\cdot OH$ was more dominant at neutral pH	Farooq *et al.* (2022)
Iron oxide/MnO_2/PS	CT	9.0	$[CT]_0 = 0.26$ mM, $[PS]_0 = 3.56$ mM, $[Catalysts]_0 = 0.25$ g/L	75%	$SO_4\cdot^-$, $\cdot OH$ and $O_2\cdot^-$ were all effectively produced, but the dominant was unknown	Jo *et al.* (2014)

active species causing CT degradation (Che & Lee 2011).

$$\cdot OH + \cdot OH \rightarrow H_2O_2 \tag{29}$$

$$\cdot OH + H_2O_2 \rightarrow HO_2\cdot + H_2O \tag{30}$$

$$SO_4\cdot^- + H_2O_2 \rightarrow HO_2\cdot + SO_4^{2-} + H^+ \tag{31}$$

$$HO_2\cdot \rightarrow O_2\cdot^- + H^+ \tag{32}$$

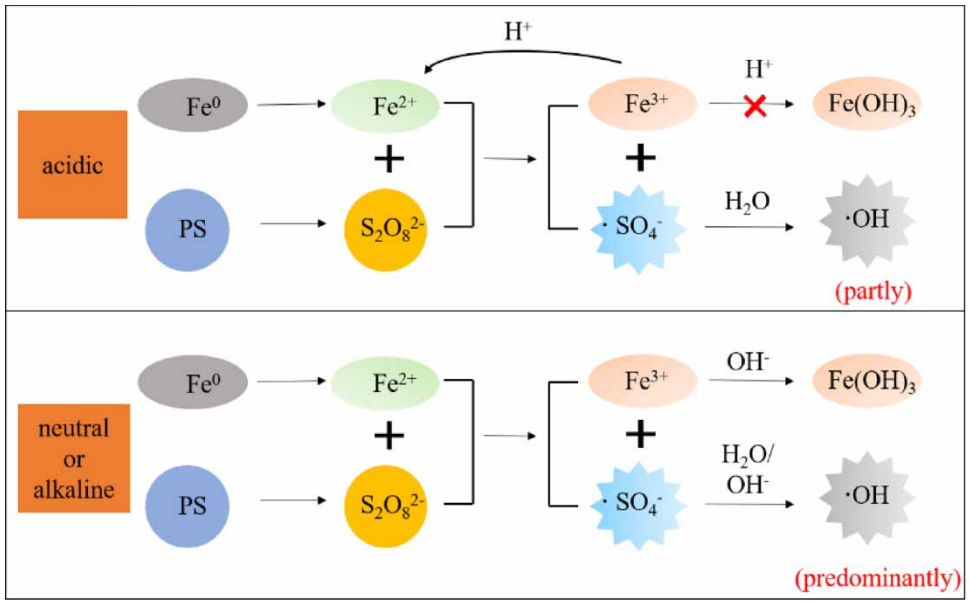

Figure 2 | Free radical reaction mechanism in the nZVI activating PS system under different pH conditions.

Besides, the generated $O_2{\cdot}^-$ can be used as a non-free radicals precursor, i.e. it can react with H_2O to produce non-free radical singlet oxygen ($^1O_2$) (Equation (33); Zhu *et al.* 2019), which can also degrade organic pollutants. In addition, the high electron transport activity of carbon-based materials makes it easier for $^1O_2$ to activate PS (Wang & Wang 2018; Yu *et al.* 2020). Duan *et al.* (2016a) found that defects at the carbon edge could directly degrade organic contaminants when PS was activated by rGO, without generating active free radicals.

$$2O_2{\cdot}^- + 2H_2O \rightarrow {}^1O_2 + H_2O_2 + 2OH^- \quad (33)$$

The non-free radical oxidation pathways found in current PS systems are mainly $^1O_2$ oxidation and electron transfer (Hu *et al.* 2017; Li *et al.* 2019). Non-free radicals have much higher selectivity than free radicals and they can resist interference from environmental factors more effectively (Ma *et al.* 2018). $^1O_2$ has a selective oxidation tendency, and it can oxidize pollutants containing electron-rich functional groups (e.g. –OH), but has difficulty in degrading pollutants with electron donating groups (e.g. –Cl, –COOH, $–NO_2$) (Hu *et al.* 2021). Therefore, degradation of CHCs mainly depends on free radicals in the system.

Just like $O_2{\cdot}^-$, $Cl{\cdot}$ is another free radical produced indirectly in the PS activation system. When CHCs are degraded by $\cdot OH$ and $SO_4{\cdot}^-$, Cl^- appears in the system due to dechlorination of free radicals. The generated Cl^- can capture $\cdot OH$ and $SO_4{\cdot}^-$ to produce $Cl{\cdot}$ (Equations (34)–(36); Wang *et al.* 2017). However, the redox potential of $Cl{\cdot}$ ($E_0 = 2.0$ V) is less than that of $SO_4{\cdot}^-$ and $\cdot OH$ (Duan *et al.* 2016b), therefore the generation of $Cl{\cdot}$ tends to reduce the oxidation capacity of the system.

$$SO_4{\cdot}^- + Cl^- \rightarrow SO_4^{2-} + Cl{\cdot} \quad (34)$$

$$\cdot OH + Cl^- \rightarrow HClO{\cdot}^- \quad (35)$$

$$HClO{\cdot}^- + H^+ \rightarrow Cl{\cdot} + H_2O \quad (36)$$

4. FACTORS AFFECTING ENGINEERING APPLICATIONS

The development of materials science is changing rapidly, the factors influencing the applications of iron-based materials activating PS are not the same. Therefore, the influencing factors in the process of removing pollutants by nZVI activating PS will be discussed from a broad perspective, rather than a specific modification technology.

4.1. Concentration of free radical

The concentration of free radicals is closely related to the concentration of PS, because PS must be activated to produce highly reactive species ($SO_4\cdot^-$) (Miserli *et al.* 2022). Studies have shown that activator concentration (Zeng *et al.* 2022), activator type (Huang *et al.* 2021; Liang *et al.* 2021; Zheng *et al.* 2021, 2022; Zhu *et al.* 2022), and activation method (Ismail *et al.* 2017; Khajeh *et al.* 2021; Satizabal-Gómez *et al.* 2021) all affect the activation of PS. These studies generally show that efficiency of pollutant removal exhibits a positive relationship with $SO_4\cdot^-$ concentration within a reasonable range, but excessive amounts affect the degradation rate. Wang *et al.* (2022) synthesized a novel porous sodalite (SOD) through reactive oxidation species from industrial waste lithium silicon fume (LSF) to stabilize nZVI. SOD@nZVI was used as an outstanding PS activator for degradation of organics. At the beginning of the reaction, with the increase of catalyst usage, more free radicals were produced and the removal rate of target pollutants increased. However, further increase of the catalyst dosage (0.4–2.0 g/L) decreased removal rate of pollutants, which was mainly caused by the self-quenching reaction of excess free radicals. Overall, the core element of pollutant degradation is free radicals, so free radicals with high activity, effective concentration and durable stability are the focus of research.

4.2. Initial pH of solution

pH is a key factor used to assess the feasibility of nZVI-based material activating PS in the *in-situ* remediation process (Yan *et al.* 2019; Rayaroth *et al.* 2020; Gao *et al.* 2021). Many studies have shown that the removal effect of organic pollutants under acidic conditions is better than that under alkaline conditions, whether in ordinary nZVI/PS systems or modified nZVI/PS systems (Liu *et al.* 2020; Zhu *et al.* 2020). The type of iron ion is significantly affected by pH value (Gao *et al.* 2021). As shown in Figure 2, H^+ can inhibit the precipitation of Fe^{3+} under acidic condition, resulting in more Fe^{2+} existing in solution and promoting the utilization efficiency of iron. In contrast, ferrous hydroxide and iron hydroxide will be formed on the surface of nZVI under alkaline or neutral condition than under acidic condition (Li *et al.* 2014b), the released Fe^{2+} will decrease and the catalytic effect will go down significantly.

Although the degradation rate of pollutants by the nZVI/PS system and the modified nZVI/PS system increased with the increase of pH, the removal effect of target pollutants in the modified nZVI/PS system was higher than that of the pure nZVI/PS system under the same pH condition. In addition, as mentioned above, pH affects the dominant active species in the system, i.e. $SO_4\cdot^-$ is more dominant in acidic conditions and $\cdot OH$ is preferred in neutral and alkaline conditions. Therefore, pH is an important factor needed to be considered in practical application.

4.3. Inorganic anions

Various inorganic anions exist in engineering applications in both groundwater and soil environments. Among them, PS systems based on $SO_4\cdot^-$ react with Cl^- and Br^- as shown in Figure 3, and the oxidation capacity of $Cl\cdot$ produced by Cl^- and $SO_4\cdot^-$ is much lower than that of $SO_4\cdot^-$ (Chan & Chu 2009). It has been confirmed that higher concentrations of Cl^-

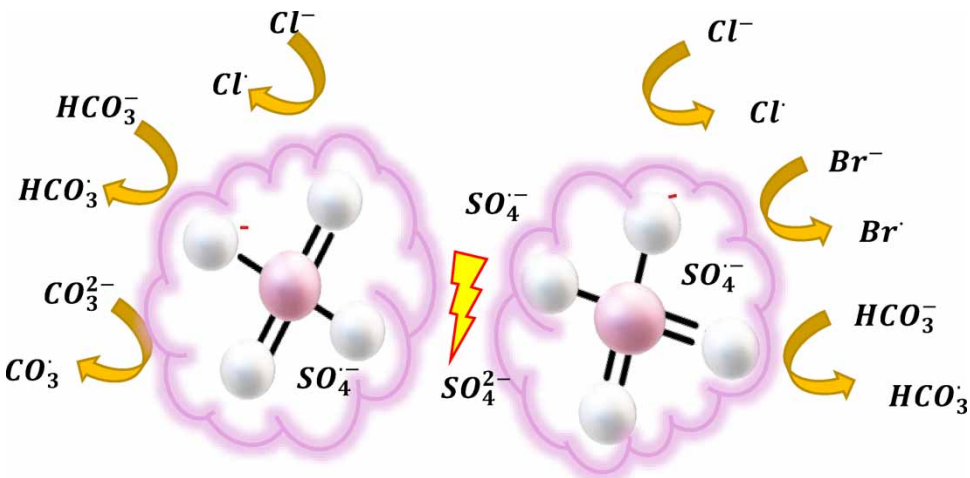

Figure 3 | Schematic diagram of influence of inorganic anions on $SO_4\cdot^-$.

showed negative effect on oxidation of TCE by PS (Liang *et al.* 2006). Other research also indicates that the consumption of free radicals by inorganic anions reduces pollutant removal efficiency (Fang *et al.* 2012; Guo *et al.* 2020; Zeng *et al.* 2022). Similar to the effect of Cl^-, HCO_3^- also exerts a significant negative effect (Liu *et al.* 2020). In addition, HCO_3^- and CO_3^{2-} are also more likely to induce the high-activity $SO_4\cdot^-$ to produce less reactive carbonate radicals. Studies have shown an overall negative impact of CO_3^{2-} and HCO_3^- on PS (Rao *et al.* 2014; Guo *et al.* 2021; Li *et al.* 2021c). In a word, $SO_4\cdot^-$ can be consumed by inorganic anions in the environment, reducing the removal efficiency of organic pollutants. This is also one of the reasons why the oxidant dosage in practical engineering applications exceeds the theoretical value greatly.

4.4. Non-target pollutants

In recent years, PS has been successively applied for *in-situ* chemical oxidation (ISCO) to repair the polluted soil and groundwater (Tsitonaki *et al.* 2010). Rayaroth *et al.* (2020) also confirmed that the proposed ISCO system was effective for the removal of mixture of pollutants such as arsenite and 1,4-dioxane. Besides CHCs, it has been shown that PS can effectively degrade multiple pollutants, such as polychlorinated biphenyls (PCBs; Fang *et al.* 2013b; Fan *et al.* 2014, 2016b), diesel fuel (Do *et al.* 2010), polycyclic aromatic hydrocarbons (PAHs; Ranc *et al.* 2016; Song *et al.* 2019; Wang *et al.* 2021), and total petroleum hydrocarbons (TPHs; Sra *et al.* 2013; Lominchar *et al.* 2018; Ossai *et al.* 2020; Zhang *et al.* 2020; Liu *et al.* 2021). A large number of previous studies have only focused on the degradation of a single pollutant, ignoring the consumption of oxidants by non-target pollutants. Recently, Xu *et al.* (2021b) conducted comprehensive remediation of organic-contaminated sites through a modified alkaline heat/persulfate (MAH/PS) system, finding that MAH/PS were more effective in degrading benzene and 1,2-dichloroethane with simple molecular configurations. The degradation efficiency of the complex pollutants such as benz[a]anthracene, benzo[a]pyrene, and TPHs was much lower. Therefore, the structural type of non-target pollutants has a significant impact on the degradation efficiency of the system.

Different activation processes involve different mechanisms for the production of free radicals. Therefore, four factors influencing the application of iron-based materials activating PS are summarized. As mentioned above, the degradation efficiency of the iron-based materials activating PS is mainly limited by the concentration of free radicals, pH, inorganic anions, and non-target pollutants. These factors require more rigorous experimental design to achieve an economical, efficient, and environmentally friendly degradation of CHCs in engineering applications.

5. CONCLUSIONS AND PROSPECTS

This paper has systematically reviewed the activation mechanism, influential factors, and treatment effects of CHCs degradation by PS activated by nZVI and its modifications. PS activated by nZVI-based materials oxidize CHCs by two types of activation: free radical oxidation ($\cdot OH$, $SO_4\cdot^-$, and $O_2\cdot^-$) and non-radical oxidation ($^1O_2$). The free radical oxidation pathway mainly relies on production of active species (especially $\cdot OH$ and $SO_4\cdot^-$) to attack the pollutants, while non-free radical oxidation is mainly completed by electrons transfer between the pollutants and the PS. Although non-free radical oxidation cannot be ignored, free radicals play a dominant role in degradation of CHCs by nZVI activating PS.

In order to overcome the weakness of nZVI, the research on nZVI modification by different ways was discussed, including supported nZVI, sulfidation, bimetallic modification, and surface-coated modification. These modification methods improve the dispersity, stability, and migration ability of nZVI in groundwater to some extent, providing theoretical supports for overcoming some drawbacks in degradation of pollutants by nZVI/PS systems. Besides, the activation properties of nZVI-based materials are affected by the concentration of free radicals, initial pH of solution, inorganic anions, and non-target pollutants in the system. A full understanding of these adverse factors will be beneficial to the practical application of modified nZVI/PS systems. Through the above analysis, it can be concluded that the application of the modified nZVI/PS system in CHCs polluted groundwater still faces some challenges.

i. Most of the advantages of modified nZVI are only exhibited under laboratory conditions. The practical application of the nZVI-based material/PS system in degradation of CHCs polluted groundwater still needs to be further verified. Besides, the high temperature, high pressure, and other harsh conditions required in the above four modification methods tend to greatly increase the use cost. Even if the modified materials can achieve better results, the acceptability of the cost needs to be reassessed.

ii. In the process of *in-situ* groundwater restoration, over-acid and over-alkali conditions will cause irreversible damage to the soil and groundwater ecosystem. In addition, it is difficult to adjust pH in the process of *in-situ* restoration. Therefore, a modified nZVI/PS system that can adapt to a wider pH range is particularly important.
iii. The composition of groundwater is complex, and various inorganic anions will consume free radicals, which greatly reduces the removal rate of CHCs. It is hard to undo its effects. Therefore, in the practical application process, the type and content of inorganic anions need to be tested in detail, although most of them do not belong to pollutants. In addition, if possible, different types of anion shielding techniques can be tried to block or delay the contact with free radicals, so that CHCs can be degraded preferentially in the system. By solving the above problems, a low-cost, high availability, and environmentally friendly modified nZVI/PS system for CHCs degradation is highly anticipated in practical engineering applications.
iv. As for the applications of the nZVI/PS system in dealing with CHCs contamination, surface pollution is relatively easy to remove because of the controllable operating conditions. By contrast, the remediation of groundwater pollution is not easy to achieve. One of the most important limiting factors is the acidic environment. The actual pH of groundwater is close to neutral in most parts of the globe, including CHC contaminated areas. Surprisingly, rapid reactions between PS and nZVI can induce acidic conditions immediately in an aquifer with high buffering capacity, making it possible for the reaction to persist. Therefore, we believe that the nZVI/PS system has a promising future in *in-situ* remediation of CHCs polluted groundwater.

ACKNOWLEDGEMENTS

The authors gratefully acknowledge financial support for this work from the Scientific research project of Tianjin North China Geological Exploration Bureau (HK2022-B1).

DATA AVAILABILITY STATEMENT

All relevant data are included in the paper or its Supplementary Information.

CONFLICT OF INTEREST

The authors declare there is no conflict.

REFERENCES

Adeleye, A. S., Keller, A. A., Miller, R. J. & Lenihan, H. S. 2013 Persistence of commercial nanoscaled zero-valent iron (nZVI) and by-products. *Journal of Nanoparticle Research: An Interdisciplinary Forum for Nanoscale Science and Technology* **15**, 1–18.

Afzal, A., Drzewicz, P., Martin, J. W. & Gamal El-Din, M. 2012 Decomposition of cyclohexanoic acid by the UV/H_2O_2 process under various conditions. *Science of The Total Environment* **426**, 387–392.

Ahmad, A., Gu, X., Li, L., Lu, S., Xu, Y. & Guo, X. 2015 Effects of pH and anions on the generation of reactive oxygen species (ROS) in nZVI-rGo-activated persulfate system. *Water, Air, & Soil Pollution* **226**, 1–12.

Al-Shamsi, M. A. & Thomson, N. R. 2013 Treatment of organic compounds by activated persulfate using nanoscale zerovalent iron. *Industrial & Engineering Chemistry Research* **52**, 13564–13571.

Anipsitakis, G. P. & Dionysiou, D. D. 2004 Radical generation by the interaction of transition metals with common oxidants. *Environmental Science & Technology* **38**, 3705–3712.

Aranzabal, A., Pereda-Ayo, B., González-Marcos, M. P., González-Marcos, J. A., López-Fonseca, R. & González-Velasco, J. R. 2014 State of the art in catalytic oxidation of chlorinated volatile organic compounds. *Chemical Papers* **68**, 1169–1186.

Ayoub, G. & Ghauch, A. 2014 Assessment of bimetallic and trimetallic iron-based systems for persulfate activation: application to sulfamethoxazole degradation. *Chemical Engineering Journal* **256**, 280–292.

Bae, S., Collins, R. N., Waite, T. D. & Hanna, K. 2018 Advances in surface passivation of nanoscale zerovalent iron: a critical review. *Environmental Science & Technology* **52**, 12010–12025.

Barzegar, G., Jorfi, S., Zarezade, V., Khatebasreh, M., Mehdipour, F. & Ghanbari, F. 2018 4-Chlorophenol degradation using ultrasound/peroxymonosulfate/nanoscale zero valent iron: reusability, identification of degradation intermediates and potential application for real wastewater. *Chemosphere* **201**, 370–379.

Bhattacharjee, S., Basnet, M., Tufenkji, N. & Ghoshal, S. 2016 Effects of rhamnolipid and carboxymethylcellulose coatings on reactivity of palladium-doped nanoscale zerovalent iron particles. *Environmental Science & Technology* **50**, 1812–1820.

Boczkaj, G. & Fernandes, A. 2017 Wastewater treatment by means of advanced oxidation processes at basic pH conditions: a review. *Chemical Engineering Journal* **320**, 608–633.

Cao, Z., Liu, X., Xu, J., Zhang, J., Yang, Y., Zhou, J., Xu, X. & Lowry, G. V. 2017 Removal of antibiotic florfenicol by sulfide-modified nanoscale zero-valent iron. *Environmental Science & Technology* **51**, 11269–11277.

Capodaglio, A. G. 2020 Critical perspective on advanced treatment processes for water and wastewater: AOPs, ARPs, and AORPs. *Applied Sciences* **10**, 45–49.

Chan, K. H. & Chu, W. 2009 Degradation of atrazine by cobalt-mediated activation of peroxymonosulfate: different cobalt counteranions in homogenous process and cobalt oxide catalysts in photolytic heterogeneous process. *Water Research* **43**, 2513–2521.

Che, H. & Lee, W. 2011 Selective redox degradation of chlorinated aliphatic compounds by Fenton reaction in pyrite suspension. *Chemosphere* **82**, 1103–1108.

Choi, H., Al-Abed, S. R., Dionysiou, D. D., Stathatos, E. & Lianos, P. 2010 Chapter 8 TiO_2-based advanced oxidation nanotechnologies for water purification and reuse. *Sustainability Science and Engineering* **2**, 229–254.

Do, S., Kwon, Y. & Kong, S. 2010 Effect of metal oxides on the reactivity of persulfate/Fe(II) in the remediation of diesel-contaminated soil and sand. *Journal of Hazardous Materials* **182**, 933–936.

Dong, H., Xie, Y., Zeng, G., Tang, L., Liang, J., He, Q., Zhao, F., Zeng, Y. & Wu, Y. 2016 The dual effects of carboxymethyl cellulose on the colloidal stability and toxicity of nanoscale zero-valent iron. *Chemosphere* **144**, 1682–1689.

Dong, H., Zhang, C., Deng, J., Jiang, Z., Zhang, L., Cheng, Y., Hou, K., Tang, L. & Zeng, G. 2018 Factors influencing degradation of trichloroethylene by sulfide-modified nanoscale zero-valent iron in aqueous solution. *Water Research* **135**, 1–10.

Dong, H., Hou, K., Qiao, W., Cheng, Y., Zhang, L., Wang, B., Li, L., Wang, Y., Ning, Q. & Zeng, G. 2019 Insights into enhanced removal of TCE utilizing sulfide-modified nanoscale zero-valent iron activated persulfate. *Chemical Engineering Journal* **359**, 1046–1055.

Dong, H., Li, Y., Wang, S., Liu, W., Zhou, G., Xie, Y. & Guan, X. 2020 Both Fe(IV) and radicals are active oxidants in the Fe(II)/peroxydisulfate process. *Environmental Science & Technology Letters* **7**, 219–224.

Duan, X., Sun, H., Kang, J., Wang, Y., Indrawirawan, S. & Wang, S. 2015 Insights into heterogeneous catalysis of persulfate activation on dimensional-structured nanocarbons. *Acs Catalysis* **5**, 4629–4636.

Duan, X., Sun, H., Ao, Z., Zhou, L., Wang, G. & Wang, S. 2016a Unveiling the active sites of graphene-catalyzed peroxymonosulfate activation. *Carbon* **107**, 371–378.

Duan, X., Su, C., Zhou, L., Sun, H., Suvorova, A., Odedairo, T., Zhu, Z., Shao, Z. & Wang, S. 2016b Surface controlled generation of reactive radicals from persulfate by carbocatalysis on nanodiamonds. *Applied Catalysis B: Environmental* **194**, 7–15.

Eljamal, R., Eljamal, O., Maamoun, I., Yilmaz, G. & Sugihara, Y. 2020 Enhancing the characteristics and reactivity of nZVI: polymers effect and mechanisms. *Journal of Molecular Liquids* **315**, 113714.

Fan, G., Cang, L., Fang, G., Qin, W., Ge, L. & Zhou, D. 2014 Electrokinetic delivery of persulfate to remediate PCBs polluted soils: effect of injection spot. *Chemosphere* **117**, 410–418.

Fan, D., Brien Johnson, O., Tratnyek, G., & Johnson, P. G. & L, R. 2016a Sulfidation of nano zerovalent iron (nZVI) for improved selectivity during in-situ chemical reduction (ISCR). *Environmental Science & Technology* **50**, 9558–9565.

Fan, G., Cang, L., Gomes, H. I. & Zhou, D. 2016b Electrokinetic delivery of persulfate to remediate PCBs polluted soils: effect of different activation methods. *Chemosphere* **144**, 138–147.

Fan, J., Gu, L., Wu, D. & Liu, Z. 2018 Mackinawite (FeS) activation of persulfate for the degradation of p-chloroaniline: surface reaction mechanism and sulfur-mediated cycling of iron species. *Chemical Engineering Journal* **333**, 657–664.

Fan, Z., Zhang, Q., Gao, B., Li, M., Liu, C. & Qiu, Y. 2019 Removal of hexavalent chromium by biochar supported nZVI composite: batch and fixed-bed column evaluations, mechanisms, and secondary contamination prevention. *Chemosphere* **217**, 85–94.

Fang, G., Dionysiou, D. D., Wang, Y., Al-Abed, S. R. & Zhou, D. 2012 Sulfate radical-based degradation of polychlorinated biphenyls: effects of chloride ion and reaction kinetics. *Journal of Hazardous Materials* **227–228**, 394–401.

Fang, G., Dionysiou, D. D., Al-Abed, S. R. & Zhou, D. 2013a Superoxide radical driving the activation of persulfate by magnetite nanoparticles: implications for the degradation of PCBs. *Applied Catalysis B: Environmental* **129**, 325–332.

Fang, G., Dionysiou, D. D., Zhou, D., Wang, Y., Zhu, X., Fan, J., Cang, L. & Wang, Y. 2013b Transformation of polychlorinated biphenyls by persulfate at ambient temperature. *Chemosphere* **90**, 1573–1580.

Fang, L., Liu, K., Li, F., Zeng, W., Hong, Z., Xu, L., Shi, Q. & Ma, Y. 2021 New insights into stoichiometric efficiency and synergistic mechanism of persulfate activation by zero-valent bimetal (Iron/Copper) for organic pollutant degradation. *Journal of Hazardous Materials* **403**, 123669.

Farooq, U., Wang, F., Shahzad, M. K., Carroll, K. C., Lyu, S. & Wang, X. 2022 Study the activation mechanism of peroxymonosulfate in iron copper systems for trichloroethane degradation. *Chemical Engineering Journal Advances* **11**, 100343.

Fatisson, J., Ghoshal, S. & Tufenkji, N. 2010 Deposition of carboxymethylcellulose-coated zero-valent iron nanoparticles onto silica: roles of solution chemistry and organic molecules. *Langmuir* **26**, 12832–12840.

Furman, O. S., Teel, A. L., Ahmad, M., Merker, M. C. & Watts, R. J. 2011 Effect of basicity on persulfate reactivity. *Journal of Environmental Engineering (New York, N.Y.)* **137**, 241–247.

Gao, Y., Champagne, P., Blair, D., He, O. & Song, T. 2020 Activated persulfate by iron-based materials used for refractory organics degradation: a review. *Water Science and Technology* **81**, 853–875.

Gao, Y., Yang, F., Jian, H., Zhen, K., Zhang, P., Tang, X., Fu, Z., Xu, W., Wang, C. & Sun, H. 2021 Pyrene degradation in an aqueous system using ferrous citrate complex activated persulfate over a wide pH range. *Journal of Environmental Chemical Engineering* **9**, 106733.

Ghauch, A., Baalbaki, A., Amasha, M., El Asmar, R. & Tantawi, O. 2017 Contribution of persulfate in UV-254 nm activated systems for complete degradation of chloramphenicol antibiotic in water. *Chemical Engineering Journal* **317**, 1012–1025.

Gong, Y. & Lin, L. 2011 Oxidative decarboxylation of levulinic acid by silver(I)/persulfate. *Molecules* **16**, 2714–2725.

Gu, X., Lu, S., Guo, X., Sima, J., Qiu, Z. & Sui, Q. 2015 Oxidation and reduction performance of 1,1,1-trichloroethane in aqueous solution by means of a combination of persulfate and zero-valent iron. *RSC Advances* **5**, 60849–60856.

Guo, W., Zhao, Q., Du, J., Wang, H., Li, X. & Ren, N. 2020 Enhanced removal of sulfadiazine by sulfidated ZVI activated persulfate process: performance, mechanisms and degradation pathways. *Chemical Engineering Journal* **388**, 124303.

Guo, J., Gao, Q., Yang, S., Zheng, F., Du, B., Wen, S. & Wang, D. 2021 Degradation of pyrene in contaminated water and soil by Fe^{2+}-activated persulfate oxidation: performance, kinetics, and background electrolytes (Cl^-, HCO_3^- and humic acid) effects. *Process Safety and Environmental Protection* **146**, 686–693.

Han, Y. & Yan, W. 2016 Reductive dechlorination of trichloroethene by zero-valent iron nanoparticles: reactivity enhancement through sulfidation treatment. *Environmental Science & Technology* **50**, 12992–13001.

Hao, J., Ji, L., Li, C., Hu, C. & Wu, K. 2018 Rapid, efficient and economic removal of organic dyes and heavy metals from wastewater by zinc-induced in-situ reduction and precipitation of graphene oxide. *Journal of the Taiwan Institute of Chemical Engineers* **88**, 137–145.

Hou, K., Pi, Z., Yao, F., Wu, B., He, L., Li, X., Wang, D., Dong, H. & Yang, Q. 2021 A critical review on the mechanisms of persulfate activation by iron-based materials: clarifying some ambiguity and controversies. *Chemical Engineering Journal* **407**, 127078.

Hu, P. & Long, M. 2016 Cobalt-catalyzed sulfate radical-based advanced oxidation: a review on heterogeneous catalysts and applications. *Applied Catalysis B: Environmental* **181**, 103–117.

Hu, P., Su, H., Chen, Z., Yu, C., Li, Q., Zhou, B., Alvarez, P. & Long, M. 2017 Selective Degradation of Organic Pollutants Using an Efficient Metal-Free Catalyst Derived from Carbonized Polypyrrole via Peroxymonosulfate Activation. *Environmental Science & Technology* **51**, 11288–11296.

Hu, M., Zhu, J. & Zhou, W. 2021 Synthesis of oxygen vacancy-enriched N/P co-doped $CoFe_2O_4$ for high-efficient degradation of organic pollutant: mechanistic insight into radical and nonradical evolution. *Environmental Pollution* **270**, 116092.

Huang, B., Lei, C., Wei, C. & Zeng, G. 2014a Chlorinated volatile organic compounds (Cl-VOCs) in environment – sources, potential human health impacts, and current remediation technologies. *Environment International* **71**, 118–138.

Huang, L., Zhou, S., Jin, F., Huang, J. & Bao, N. 2014b Characterization and mechanism analysis of activated carbon fiber felt-stabilized nanoscale zero-valent iron for the removal of Cr(VI) from aqueous solution. *Colloids and Surfaces A: Physicochemical and Engineering Aspects* **447**, 59–66.

Huang, Z., Yao, Y., Lu, J., Chen, C., Lu, W., Huang, S. & Chen, W. 2016 The consortium of heterogeneous cobalt phthalocyanine catalyst and bicarbonate ion as a novel platform for contaminants elimination based on peroxymonosulfate activation. *Journal of Hazardous Materials* **301**, 214–221.

Huang, J., Yi, S., Zheng, C. & Lo, I. 2019 Persulfate activation by natural zeolite supported nanoscale zero-valent iron for trichloroethylene degradation in groundwater. *Science of the Total Environment* **684**, 351–359.

Huang, W., Xiao, S., Zhong, H., Yan, M. & Yang, X. 2021 Activation of persulfates by carbonaceous materials: a review. *Chemical Engineering Journal* **418**, 129297.

Hussain, I., Li, M., Zhang, Y., Li, Y., Huang, S., Du, X., Liu, G., Hayat, W. & Anwar, N. 2017 Insights into the mechanism of persulfate activation with nZVI/BC nanocomposite for the degradation of nonylphenol. *Chemical Engineering Journal* **311**, 163–172.

Idrees, A., Shan, A., Ali, M., Abbas, Z., Shahzad, T., Hussain, S., Mahmood, F., Farooq, U., Danish, M. & Lyu, S. 2021 Highly efficient degradation of trichloroethylene in groundwater based on persulfate activation by polyvinylpyrrolidone functionalized Fe/Cu bimetallic nanoparticles. *Journal of Environmental Chemical Engineering* **9**, 105341.

Ikea, I. A., Linden, K. G., Orbell, J. D. & Duke, M. 2018 Critical review of the science and sustainability of persulphate advanced oxidation processes. *Chemical Engineering Journal* **33**, 651–669.

Ismail, L., Ferronato, C., Fine, L., Jaber, F. & Chovelon, J. 2017 Elimination of sulfaclozine from water with $SO_4{\cdot}^-$ radicals: evaluation of different persulfate activation methods. *Applied Catalysis B: Environmental* **201**, 573–581.

Jiemvarangkul, P., Zhang, W. & Lien, H. 2011 Enhanced transport of polyelectrolyte stabilized nanoscale zero-valent iron (nZVI) in porous media. *Chemical Engineering Journal* **170**, 482–491.

Jin, Q., Chen, Q., Kang, J., Shen, J., Guo, F. & Chen, Z. 2020 Fabrication of iron-dipicolinamide catalyst with Fe-N bonds for enhancing non-radical reactive species under alkaline Fenton process. *Chemosphere* **241**, 125005.

Jo, Y., Do, S. & Kong, S. 2014 Persulfate activation by iron oxide-immobilized MnO_2 composite: identification of iron oxide and the optimum pH for degradations. *Chemosphere* **95**, 550–555.

Khajeh, M., Amin, M. M., Fatehizadeh, A. & Aminabhavi, T. M. 2021 Synergetic degradation of atenolol by hydrodynamic cavitation coupled with sodium persulfate as zero-waste discharge process: effect of coexisting anions. *Chemical Engineering Journal* **416**, 129163.

Kim, E. J., Kim, J. H., Azad, A. M. & Chang, Y. S. 2011 Facile synthesis and characterization of Fe/FeS nanoparticles for environmental applications. *ACS Applied Materials & Interfaces* **3**, 1457–1462.

Kim, C., Ahn, J. Y., Kim, T. Y., Shin, W. S. & Hwang, I. 2018 Activation of persulfate by nanosized zero-valent iron (NZVI): mechanisms and transformation products of NZVI. *Environmental Science & Technology* **52**, 3625–3633.

Kueper, B. H., Abbott, W. & Farquhar, G. 1989 Experimental observations of multiphase flow in heterogeneous porous media. *Journal of Contaminant Hydrology* **5**, 83–95.

Kusic, H., Peternel, I., Koprivanac, N. & Loncaric Bozic, A. 2011 Iron-activated persulfate oxidation of an azo dye in model wastewater: influence of iron activator type on process optimization. *Journal of Environmental Engineering (New York, N.Y.)* **137**, 454–463.

Lai, B., Chen, Z., Zhou, Y., Yang, P., Wang, J. & Chen, Z. 2013 Removal of high concentration p-nitrophenol in aqueous solution by zero valent iron with ultrasonic irradiation (US–ZVI). *Journal of Hazardous Materials* **250–251**, 220–228.

Lefevre, E., Bossa, N., Wiesner, M. R. & Gunsch, C. K. 2016 A review of the environmental implications of in situ remediation by nanoscale zero valent iron (nZVI): behavior, transport and impacts on microbial communities. *Science of the Total Environment* **565**, 889–901.

Lei, Y., Chen, C. S., Tu, Y. J., Huang, Y. H. & Zhang, H. 2015 Heterogeneous degradation of organic pollutants by persulfate activated by CuO-Fe_3O_4: mechanism, stability, and effects of pH and bicarbonate ions. *Environmental Science & Technology* **49**, 6838–6845.

Li, Y., Zhang, Y., Li, J. & Zheng, X. 2011 Enhanced removal of pentachlorophenol by a novel composite: nanoscale zero valent iron immobilized on organobentonite. *Environmental Pollution* **159**, 3744–3749.

Li, H., Wan, J., Ma, Y., Huang, M., Wang, Y. & Chen, Y. 2014a New insights into the role of zero-valent iron surface oxidation layers in persulfate oxidation of dibutyl phthalate solutions. *Chemical Engineering Journal* **250**, 137–147.

Li, H., Wan, J., Ma, Y., Wang, Y. & Huang, M. 2014b Influence of particle size of zero-valent iron and dissolved silica on the reactivity of activated persulfate for degradation of acid orange 7. *Chemical Engineering Journal* **237**, 487–496.

Li, D., Mao, Z., Zhong, Y., Huang, W., Wu, Y. & Peng, P. 2016 Reductive transformation of tetrabromobisphenol A by sulfidated nano zerovalent iron. *Water Research* **103**, 1–9.

Li, J., Zhang, X., Sun, Y., Liang, L., Pan, B., Zhang, W. & Guan, X. 2017 Advances in sulfidation of zerovalent iron for water decontamination. *Environmental Science & Technology* **51**, 13533–13544.

Li, H., Shan, C. & Pan, B. 2019 Development of Fe-doped g-c3n4/graphite mediated peroxymonosulfate activation for degradation of aromatic pollutants via nonradical pathway. *Science of The Total Environment* **675**, 62–72.

Li, S., Tang, J., Liu, Q., Liu, X. & Gao, B. 2020 A novel stabilized carbon-coated nZVI as heterogeneous persulfate catalyst for enhanced degradation of 4-chlorophenol. *Environment International* **138**, 105639.

Li, H., Si, R., Wang, W., Huang, Y., Xiang, M., Wang, C., Chen, S., Cao, W., Lu, Z. & Huang, M. 2021a Sulfidated nanoscale zero-valent iron dispersed in dendritic mesoporous silica nanospheres for degrading tetrabromobisphenol A. *Colloids and Surfaces A: Physicochemical and Engineering Aspects* **621**, 126586.

Li, X., Shen, J., Sun, Z., Liu, Y., Zhang, W., Wu, B., Ma, F. & Gu, Q. 2021b Degradation of 2,4-dinitrotoluene using ferrous activated persulfate: kinetics, mechanisms, and effects of natural water matrices. *Journal of Environmental Chemical Engineering* **9**, 106048.

Li, Y., Zhao, H. & Zhu, L. 2021c Remediation of soil contaminated with organic compounds by nanoscale zero-valent iron: a review. *Science of the Total Environment* **760**, 143413.

Lian, W., Yi, X., Huang, K., Tang, T., Wang, R., Tao, X., Zheng, Z., Dang, Z., Yin, H. & Lu, G. 2019 Degradation of tris(2-chloroethyl) phosphate (TCEP) in aqueous solution by using pyrite activating persulfate to produce radicals. *Ecotoxicology and Environmental Safety* **174**, 667–674.

Liang, C. & Lai, M. 2008 Trichloroethylene degradation by zero valent iron activated persulfate oxidation. *Environmental Engineering Science* **25**, 1071–1077.

Liang, C., Bruell, C. J., Marley, M. C. & Sperry, K. L. 2004 Persulfate oxidation for in situ remediation of TCE. I. Activated by ferrous ion with and without a persulfate–thiosulfate redox couple. *Chemosphere* **55**, 1213–1223.

Liang, C., Wang, Z. & Mohanty, N. 2006 Influences of carbonate and chloride ions on persulfate oxidation of trichloroethylene at 20 °C. *Science of The Total Environment* **370**, 271–277.

Liang, H., Zhang, Y., Huang, S. & Hussain, I. 2013 Oxidative degradation of p-chloroaniline by copper oxidate activated persulfate. *Chemical Engineering Journal* **218**, 384–391.

Liang, D. W., Yang, Y. H., Xu, W. W., Peng, S. K., Lu, S. F. & Xiang, Y. 2014 Nonionic surfactant greatly enhances the reductive debromination of polybrominated diphenyl ethers by nanoscale zero-valent iron: mechanism and kinetics. *Journal of Hazardous Materials* **278**, 592–596.

Liang, J., Duan, X., Xu, X., Chen, K., Wu, F., Qiu, H., Liu, C., Wang, S. & Cao, X. 2021 Biomass-derived pyrolytic carbons accelerated Fe(III)/Fe(II) redox cycle for persulfate activation: pyrolysis temperature-depended performance and mechanisms. *Applied Catalysis B: Environmental* **297**, 120446.

Liu, J., Liu, A. & Zhang, W. 2016a The influence of polyelectrolyte modification on nanoscale zero-valent iron (nZVI): aggregation, sedimentation, and reactivity with Ni(II) in water. *Chemical Engineering Journal* **303**, 268–274.

Liu, Z., Zhang, F., Hoekman, S. K., Liu, T., Gai, C. & Peng, N. 2016b Homogeneously dispersed zerovalent iron nanoparticles supported on hydrochar-derived porous carbon: simple, in situ synthesis and use for dechlorination of PCBs. *ACS Sustainable Chemistry & Engineering* **4**, 3261–3267.

Liu, Y., Zhang, Y., Wang, B., Wang, S., Liu, M., Wu, Y., Lu, L., Ren, H., Li, H., Dong, W. & Qadeer, A. 2020 Degradation of ibuprofen in soil systems by persulfate activated with pyrophosphate chelated Fe(II). *Chemical Engineering Journal* **379**, 122145.

Liu, J., Wei, K., Xu, S., Cui, J., Ma, J., Xiao, X., Xi, B. & He, X. 2021 Surfactant-enhanced remediation of oil-contaminated soil and groundwater: a review. *Science of The Total Environment* **756**, 144142.

Lominchar, M. A., Santos, A., de Miguel, E. & Romero, A. 2018 Remediation of aged diesel contaminated soil by alkaline activated persulfate. *Science of The Total Environment* **622–623**, 41–48.

Ma, W., Wang, N., Fan, Y., Tong, T., Han, X. & Du, Y. 2018 Non-radical-dominated catalytic degradation of bisphenol A by ZIF-67 derived nitrogen-doped carbon nanotubes frameworks in the presence of peroxymonosulfate. *Chemical Engineering Journal* **336**, 721–731.

Ma, X., Rao, T., Zhao, M., Jia, Z., Ren, G., Liu, J., Guo, H., Wu, Z. & Xie, H. 2022 A novel induced zero-valent iron electrode for in-situ slow release of Fe^{2+} to effectively trigger electro-Fenton oxidation under neutral pH condition: advantages and mechanisms. *Separation and Purification Technology* **283**, 120160.

Mandal, S., Pu, S., Shangguan, L., Liu, S., Ma, H., Adhikari, S. & Hou, D. 2020 Synergistic construction of green tea biochar supported nZVI for immobilization of lead in soil: a mechanistic investigation. *Environment International* **135**, 105374.

Mangayayam, M., Dideriksen, K., Ceccato, M. & Tobler, D. J. 2019 The structure of sulfidized zero-valent iron by one-pot synthesis: impact on contaminant selectivity and long-term performance. *Environmental Science & Technology* **53**, 4389–4396.

Mangayayam, M. C., Alonso-de-Linaje, V., Dideriksen, K. & Tobler, D. J. 2020 Effects of common groundwater ions on the transformation and reactivity of sulfidized nanoscale zerovalent iron. *Chemosphere* **249**, 126137.

Matzek, L. W. & Carter, K. E. 2016 Activated persulfate for organic chemical degradation: a review. *Chemosphere (Oxford)* **151**, 178–188.

Miserli, K., Kogola, D., Paraschoudi, I. & Konstantinou, I. 2022 Activation of persulfate by biochar for the degradation of phenolic compounds in aqueous systems. *Chemical Engineering Journal Advances* **9**, 100201.

Moreira, F. C., Boaventura, R. A. R., Brillas, E. & Vilar, V. J. P. 2017 Electrochemical advanced oxidation processes: a review on their application to synthetic and real wastewaters. *Applied Catalysis B: Environmental* **202**, 217–261.

Nunez, G. A., Boparai, H. K. & O'Carroll, D. M. 2016 Enhanced dechlorination of 1,2-dichloroethane by coupled nano iron-dithionite treatment. *Environmental Science & Technology* **50**, 5243–5251.

Oh, S. Y., Kim, H. W., Park, J. M., Park, H. S. & Yoon, C. 2009 Oxidation of polyvinyl alcohol by persulfate activated with heat, Fe^{2+}, and zero-valent iron. *Journal of Hazardous Materials* **168**, 346–351.

Oh, S. Y., Kang, S. G. & Chiu, P. C. 2010 Degradation of 2,4-dinitrotoluene by persulfate activated with zero-valent iron. *Science of the Total Environment* **408**, 3464–3468.

Oh, W., Dong, Z. & Lim, T. 2016 Generation of sulfate radical through heterogeneous catalysis for organic contaminants removal: current development, challenges and prospects. *Applied Catalysis B: Environmental* **194**, 169–201.

Olmez-Hanci, T. & Arslan-Alaton, I. 2013 Comparison of sulfate and hydroxyl radical based advanced oxidation of phenol. *Chemical Engineering Journal* **224**, 10–16.

Ossai, I. C., Ahmed, A., Hassan, A. & Hamid, F. S. 2020 Remediation of soil and water contaminated with petroleum hydrocarbon: a review. *Environmental Technology & Innovation* **17**, 100526.

Oturan, M. A. & Aaron, J. 2014 Advanced oxidation processes in water/wastewater treatment: principles and applications: a review. *Critical Reviews in Environmental Science and Technology* **44**, 2577–2641.

Parenky, A. C., de Souza, N. G., Nguyen, H. H., Junha Jeon, P. D. & Hyeok Choi, P. D. 2020 Decomposition of carboxylic PFAS by persulfate activated by silver under ambient conditions. *Journal of Environmental Engineering* **146**, 10.

Pera-Titus, M., García-Molina, V., Baños, M. A., Giménez, J. & Esplugas, S. 2004 Degradation of chlorophenols by means of advanced oxidation processes: a general review. *Applied Catalysis. B, Environmental* **47**, 219–256.

Popescu, I. A., Varga, T., Egedy, A., Fogarasi, S., Chován, T., Imre-Lucaci, Á. & Ilea, P. 2015 Kinetic models based on analysis of the dissolution of copper, zinc and brass from WEEE in a sodium persulfate environment. *Computers & Chemical Engineering* **83**, 214–220.

Qi, C., Liu, X., Lin, C., Zhang, X., Ma, J., Tan, H. & Ye, W. 2014 Degradation of sulfamethoxazole by microwave-activated persulfate: kinetics, mechanism and acute toxicity. *Chemical Engineering Journal* **249**, 6–14.

Qu, G., Chu, R., Wang, H., Wang, T., Zhang, Z., Qiang, H., Liang, D. & Hu, S. 2020 Simultaneous removal of chromium(VI) and tetracycline hydrochloride from simulated wastewater by nanoscale zero-valent iron/copper-activated persulfate. *Environmental Science and Pollution Research* **27**, 40826–40836.

Rajajayavel, S. R. C. & Ghoshal, S. 2015 Enhanced reductive dechlorination of trichloroethylene by sulfidated nanoscale zerovalent iron. *Water Research* **78**, 144–153.

Ranc, B., Faure, P., Croze, V. & Simonnot, M. O. 2016 Selection of oxidant doses for in situ chemical oxidation of soils contaminated by polycyclic aromatic hydrocarbons (PAHs): a review. *Journal of Hazardous Materials* **312**, 280–297.

Rao, Y. F., Qu, L., Yang, H. & Chu, W. 2014 Degradation of carbamazepine by Fe(II)-activated persulfate process. *Journal of Hazardous Materials* **268**, 23–32.

Rastogi, A., Al-Abed, S. R. & Dionysiou, D. D. 2009 Effect of inorganic, synthetic and naturally occurring chelating agents on Fe(II) mediated advanced oxidation of chlorophenols. *Water Research (Oxford)* **43**, 684–694.

Ravikumar, K. V. G., Santhosh, S., Sudakaran, S. V., Nancharaiah, Y. V. P., Mrudula, P., Chandrasekaran, N. & Mukherjee, A. 2018 Biogenic nano zero valent iron (Bio-nZVI) anaerobic granules for textile dye removal. *Journal of Environmental Chemical Engineering* **6**, 1683–1689.

Rayaroth, M. P., Lee, C., Aravind, U. K., Aravindakumar, C. T. & Chang, Y. 2017 Oxidative degradation of benzoic acid using Fe^0- and sulfidized Fe^0-activated persulfate: a comparative study. *Chemical Engineering Journal* **315**, 426–436.

Rayaroth, M. P., Oh, D., Lee, C., Kang, Y. & Chang, Y. 2020 In situ chemical oxidation of contaminated groundwater using a sulfidized nanoscale zerovalent iron–persulfate system: insights from a box-type study. *Chemosphere* **257**, 127117.

Ren, G., Li, R., Zhao, M., Hou, Q., Rao, T., Zhou, M. & Ma, X. 2023 Membrane electrodes for electrochemical advanced oxidation processes: preparation, self-cleaning mechanisms and prospects. *Chemical Engineering Journal* **451**, 138907.

Rodriguez, S., Vasquez, L., Romero, A. & Santos, A. 2014 Dye oxidation in aqueous phase by using zero-valent iron as persulfate activator: kinetic model and effect of particle size. *Industrial & Engineering Chemistry Research* **53**, 12288–12294.

Saha, A. K., Sinha, A. & Pasupuleti, S. 2019 Modification, characterization and investigations of key factors controlling the transport of modified nano zero-valent iron (nZVI) in porous media. *Environmental Technology* **40**, 1543–1556.

Satizabal-Gómez, V., Collazos-Botero, M. A., Serna-Galvis, E. A., Torres-Palma, R. A., Bravo-Suárez, J. J., Machuca-Martínez, F. & Castilla-Acevedo, S. F. 2021 Effect of the presence of inorganic ions and operational parameters on free cyanide degradation by ultraviolet C activation of persulfate in synthetic mining wastewater. *Minerals Engineering* **170**, 107031.

Shan, A., Idrees, A., Zaman, W. Q., Abbas, Z., Ali, M., Rehman, M. S. U., Hussain, S., Danish, M., Gu, X. & Lyu, S. 2021a Synthesis of nZVI-Ni@BC composite as a stable catalyst to activate persulfate: trichloroethylene degradation and insight mechanism. *Journal of Environmental Chemical Engineering* **9**, 104808.

Shan, A., Idrees, A., Zaman, W. Q., Abbas, Z., Farooq, U., Ali, M., Yang, R., Zeng, G., Danish, M., Gu, X. & Lyu, S. 2021b Enhancement in reactivity via sulfidation of FeNi@BC for efficient removal of trichloroethylene: insight mechanism and the role of reactive oxygen species. *Science of The Total Environment* **794**, 148674.

Shi, J., Long, C. & Li, A. 2016 Selective reduction of nitrate into nitrogen using Fe–Pd bimetallic nanoparticle supported on chelating resin at near-neutral pH. *Chemical Engineering Journal* **286**, 408–415.

Shokoohi, R., Bajalan, S., Salari, M., Shabanloo, A., Gołaś, J., Zarębska, K., Marczak, M., Szramowiat-Sala, K. & Nosek, K. 2019 Thermochemical degradation of furfural by sulfate radicals in aqueous solution: optimization and synergistic effect studies. *Environmental Science and Pollution Research International* **26**, 8914–8927.

Song, S., Su, Y., Adeleye, A. S., Zhang, Y. & Zhou, X. 2017 Optimal design and characterization of sulfide-modified nanoscale zerovalent iron for diclofenac removal. *Applied Catalysis B: Environmental* **201**, 211–220.

Song, Y., Fang, G., Zhu, C., Zhu, F., Wu, S., Chen, N., Wu, T., Wang, Y., Gao, J. & Zhou, D. 2019 Zero-valent iron activated persulfate remediation of polycyclic aromatic hydrocarbon-contaminated soils: an in situ pilot-scale study. *Chemical Engineering Journal* **355**, 65–75.

Soukupova, J., Zboril, R., Medrik, I., Filip, J., Safarova, K., Ledl, R., Mashlan, M., Nosek, J. & Cernik, M. 2015 Highly concentrated, reactive and stable dispersion of zero-valent iron nanoparticles: direct surface modification and site application. *Chemical Engineering Journal* **262**, 813–822.

Sra, K. S., Thomson, N. R. & Barker, J. F. 2013 Persulfate injection into a gasoline source zone. *Journal of Contaminant Hydrology* **150**, 35–44.

Su, H., Fang, Z., Tsang, P. E., Zheng, L., Cheng, W., Fang, J. & Zhao, D. 2016 Remediation of hexavalent chromium contaminated soil by biochar-supported zero-valent iron nanoparticles. *Journal of Hazardous Materials* **318**, 533–540.

Sun, M., Cheng, G., Ge, X., Chen, M., Wang, C., Lou, L. & Xu, X. 2018 Aqueous Hg(II) immobilization by chitosan stabilized magnetic iron sulfide nanoparticles. *Science of the Total Environment* **621**, 1074–1083.

Sun, Y., Li, M., Gu, X., Danish, M., Shan, A., Ali, M., Qiu, Z., Sui, Q. & Lyu, S. 2021 Mechanism of surfactant in trichloroethene degradation in aqueous solution by sodium persulfate activated with chelated-Fe(II). *Journal of Hazardous Materials* **407**, 124814.

Tan, X. F., Liu, Y. G., Gu, Y. L., Xu, Y., Zeng, G. M., Hu, X. J., Liu, S. B., Wang, X., Liu, S. M. & Li, J. 2016 Biochar-based nano-composites for the decontamination of wastewater: a review. *Bioresource Technology* **212**, 318–333.

Tesh, S. J. & Scott, T. B. 2014 Nano-composites for water remediation: a review. *Advanced Materials* **26**, 6056–6068.

Tsitonaki, A., Petri, B., Crimi, M., Mosbaek, H., Siegrist, R. L. & Bjerg, P. L. 2010 In situ chemical oxidation of contaminated soil and groundwater using persulfate: a review. *Critical Reviews in Environmental Science and Technology* **40**, 55–91.

Wacławek, S., Lutze, H. V., Grübel, K., Padil, V. V. T., Černík, M. & Dionysiou, D. D. 2017 Chemistry of persulfates in water and wastewater treatment: a review. *Chemical Engineering Journal* **330**, 44–62.

Wang, J. & Wang, S. 2018 Activation of persulfate (PS) and peroxymonosulfate (PMS) and application for the degradation of emerging contaminants. *Chemical Engineering Journal* **334**, 1502–1517.

Wang, Y., Sun, H., Duan, X., Ang, H. M., Tadé, M. O. & Wang, S. 2015 A new magnetic nano zero-valent iron encapsulated in carbon spheres for oxidative degradation of phenol. *Applied Catalysis B: Environmental* **172–173**, 73–81.

Wang, Y., Cao, D. & Zhao, X. 2017 Heterogeneous degradation of refractory pollutants by peroxymonosulfate activated by CoO_x-doped ordered mesoporous carbon. *Chemical Engineering Journal* **328**, 1112–1121.

Wang, Z., Jiang, J., Pang, S., Zhou, Y., Guan, C., Gao, Y., Li, J., Yang, Y., Qiu, W. & Jiang, C. 2018 Is sulfate radical really generated from peroxydisulfate activated by iron(II) for environmental decontamination? *Environmental Science & Technology* **52**, 11276–11284.

Wang, J., Duan, X., Dong, Q., Meng, F., Tan, X., Liu, S. & Wang, S. 2019a Facile synthesis of N-doped 3D graphene aerogel and its excellent performance in catalytic degradation of antibiotic contaminants in water. *Carbon (New York)* **144**, 781–790.

Wang, Z., Qiu, W., Pang, S., Zhou, Y., Gao, Y., Guan, C. & Jiang, J. 2019b Further understanding the involvement of Fe(IV) in peroxydisulfate and peroxymonosulfate activation by Fe(II) for oxidative water treatment. *Chemical Engineering Journal* **371**, 842–847.

Wang, Z., Qiu, W., Pang, S., Gao, Y., Zhou, Y., Cao, Y. & Jiang, J. 2020 Relative contribution of ferryl ion species (Fe(IV)) and sulfate radical formed in nanoscale zero valent iron activated peroxydisulfate and peroxymonosulfate processes. *Water Research* **172**, 115504.

Wang, J., Zhang, X., Zhou, X., Waigi, M. G., Gudda, F. O., Zhang, C. & Ling, W. 2021 Promoted oxidation of polycyclic aromatic hydrocarbons in soils by dual persulfate/calcium peroxide system. *Science of The Total Environment* **758**, 143680.

Wang, Y., Armutlulu, A., Lin, H., Wu, M., Zhang, W., Xie, R. & Lai, B. 2022 Novel sodalite stabilized zero-valent iron for super stable and outstanding efficiency in activating persulfate for organic pollutants fast removal. *Science of The Total Environment* **825**, 153893.

Wei, X., Gao, N., Li, C., Deng, Y., Zhou, S. & Li, L. 2016 Zero-valent iron (ZVI) activation of persulfate (PS) for oxidation of bentazon in water. *Chemical Engineering Journal* **285**, 660–670.

Wei, D., Li, B., Huang, H., Luo, L., Zhang, J., Yang, Y., Guo, J., Tang, L., Zeng, G. & Zhou, Y. 2018 Biochar-based functional materials in the purification of agricultural wastewater: fabrication, application and future research needs. *Chemosphere* **197**, 165–180.

Wu, X., Gu, X., Lu, S., Qiu, Z., Sui, Q., Zang, X., Miao, Z. & Xu, M. 2015 Strong enhancement of trichloroethylene degradation in ferrous ion activated persulfate system by promoting ferric and ferrous ion cycles with hydroxylamine. *Separation and Purification Technology* **147**, 186–193.

Wu, S., He, H., Li, X., Yang, C., Zeng, G., Wu, B., He, S. & Lu, L. 2018a Insights into atrazine degradation by persulfate activation using composite of nanoscale zero-valent iron and graphene: performances and mechanisms. *Chemical Engineering Journal* **341**, 126–136.

Wu, C., Yang, M. & Lin, K. A. 2018b Magnetic Co/Fe nanohybrid supported on carbonaceous marcosphere as a heterogeneous catalyst for sulfate radical-based chemical oxidation. *Journal of Environmental Chemical Engineering* **6**, 426–434.

Wu, Y., Chen, X., Han, Y., Yue, D., Cao, X., Zhao, Y. & Qian, X. 2019 Highly efficient utilization of nano-Fe(0) embedded in mesoporous carbon for activation of peroxydisulfate. *Environmental Science & Technology* **53**, 9081–9090.

Xie, Y. & Cwiertny, D. M. 2010 Use of dithionite to extend the reactive lifetime of nanoscale zero-valent iron treatment systems. *Environmental Science & Technology* **44**, 8649–8655.

Xiong, Z., Lai, B., Yang, P., Zhou, Y., Wang, J. & Fang, S. 2015 Comparative study on the reactivity of Fe/Cu bimetallic particles and zero valent iron (ZVI) under different conditions of N_2, air or without aeration. *Journal of Hazardous Materials* **297**, 261–268.

Xu, H., Tian, W., Zhang, Y., Tang, J., Zhao, Z. & Chen, Y. 2018 Reduced graphene oxide/attapulgite-supported nanoscale zero-valent iron removal of acid Red 18 from aqueous solution. *Water, Air, & Soil Pollution* **229**, 1–16.

Xu, J., Cao, Z., Wang, Y., Zhang, Y., Gao, X., Ahmed, M. B., Zhang, J., Yang, Y., Zhou, J. L. & Lowry, G. V. 2019a Distributing sulfidized nanoscale zerovalent iron onto phosphorus-functionalized biochar for enhanced removal of antibiotic florfenicol. *Chemical Engineering Journal* **359**, 713–722.

Xu, J., Cao, Z., Zhou, H., Lou, Z., Wang, Y., Xu, X. & Lowry, G. V. 2019b Sulfur dose and sulfidation time affect reactivity and selectivity of post-sulfidized nanoscale zerovalent iron. *Environmental Science & Technology* **53**, 13344–13352.

Xu, Z., Huang, J., Fu, R., Zhou, Z., Ali, M., Shan, A., Yang, R., Zeng, G., Zhou, Z., Idrees, A. & Lyu, S. 2021a Enhanced trichloroethylene degradation in the presence of surfactant: pivotal role of Fe(II)/nZVI catalytic synergy in persulfate system. *Separation and Purification Technology* **272**, 118885.

Xu, Q., Shi, F., You, H. & Wang, S. 2021b Integrated remediation for organic-contaminated site by forcing running-water to modify alkali-heat/persulfate via oxidation process transfer. *Chemosphere* **262**, 128352.

Yan, W., Lien, H. L., Koel, B. E. & Zhang, W. X. 2013 Iron nanoparticles for environmental clean-up: recent developments and future outlook. *Environmental Science-Processes & Impacts* **15**, 63–77.

Yan, J., Han, L., Gao, W., Xue, S. & Chen, M. 2015 Biochar supported nanoscale zerovalent iron composite used as persulfate activator for removing trichloroethylene. *Bioresource Technology* **175**, 269–274.

Yan, J., Gao, W., Dong, M., Han, L., Qian, L., Nathanail, C. P. & Chen, M. 2016 Degradation of trichloroethylene by activated persulfate using a reduced graphene oxide supported magnetite nanoparticle. *Chemical Engineering Journal* **295**, 309–316.

Yan, S., Zhang, X. & Zhang, H. 2019 Persulfate activation by Fe(III) with bioelectricity at acidic and near-neutral pH regimes: homogeneous versus heterogeneous mechanism. *Journal of Hazardous Materials* **374**, 92–100.

Yang, S., Wang, P., Yang, X., Wei, G., Zhang, W. & Shan, L. 2009 A novel advanced oxidation process to degrade organic pollutants in wastewater: microwave-activated persulfate oxidation. *Journal of Environmental Sciences* **21**, 1175–1180.

Yang, L., Gao, J., Liu, Y., Zhang, Z., Zou, M., Liao, Q. & Shang, J. 2018 Removal of methyl orange from water using sulfur-modified nZVI supported on biochar composite. *Water, Air, & Soil Pollution* **229**, 355.

Yu, P., Yu, H., Sun, Q. & Ma, B. 2019 Filter paper supported nZVI for continuous treatment of simulated dyeing wastewater. *Scientific Reports* **9**, 11322.

Yu, J., Feng, H., Tang, L., Pang, Y., Zeng, G., Lu, Y., Dong, H., Wang, J., Liu, Y., Feng, C., Wang, J., Peng, B. & Ye, S. 2020 Metal-free carbon materials for persulfate-based advanced oxidation process: Microstructure, property and tailoring. *Progress in Materials Science* **111**, 100654.

Yuan, S., Liao, P. & Alshawabkeh, A. N. 2014 Electrolytic manipulation of persulfate reactivity by iron electrodes for trichloroethylene degradation in groundwater. *Environmental Science & Technology* **48**, 656–663.

Yuan, Y., Tao, H., Fan, J. & Ma, L. 2015 Degradation of p-chloroaniline by persulfate activated with ferrous sulfide ore particles. *Chemical Engineering Journal* **268**, 38–46.

Zeng, Y., Walker, H. & Zhu, Q. 2017 Reduction of nitrate by NaY zeolite supported Fe, Cu/Fe and Mn/Fe nanoparticles. *Journal of Hazardous Materials* **324**, 605–616.

Zeng, X., Wang, L., Zhang, Y., Zhou, S., Yu, Z., Liu, X. & Chen, C. 2022 Enhanced removal of organic pollutants by ball-milled FeS/ZVI activated persulfate process: characterization, performance, and mechanisms. *Surfaces and Interfaces* **29**, 101697.

Zhang, M., Chen, X., Zhou, H., Murugananthan, M. & Zhang, Y. 2015 Degradation of p-nitrophenol by heat and metal ions co-activated persulfate. *Chemical Engineering Journal* **264**, 39–47.

Zhang, P., Yuan, S. & Liao, P. 2016 Mechanisms of hydroxyl radical production from abiotic oxidation of pyrite under acidic conditions. *Geochimica et Cosmochimica Acta* **172**, 444–457.

Zhang, B., Guo, Y., Huo, J., Xie, H., Xu, C. & Liang, S. 2020 Combining chemical oxidation and bioremediation for petroleum polluted soil remediation by BC-nZVI activated persulfate. *Chemical Engineering Journal* **382**, 123055.

Zhang, W., Qian, L., Han, L., Yang, L., Ouyang, D., Long, Y., Wei, Z., Dong, X., Liang, C., Li, J., Gu, M. & Chen, M. 2022 Synergistic roles of Fe(II) on simultaneous removal of hexavalent chromium and trichloroethylene by attapulgite-supported nanoscale zero-valent iron/persulfate system. *Chemical Engineering Journal* **430**, 132841.

Zhao, X., Liu, W., Cai, Z., Han, B., Qian, T. & Zhao, D. 2016 An overview of preparation and applications of stabilized zero-valent iron nanoparticles for soil and groundwater remediation. *Water Research* **100**, 245–266.

Zheng, N., He, X., Hu, R., Guo, W. & Hu, Z. 2021 Co-activation of persulfate by cation and anion from FeP for advanced oxidation processes. *Applied Catalysis B: Environmental* **298**, 120505.

Zheng, X., Xu, T., Kang, X., Xing, Y., Cao, Y. & Gui, X. 2022 Structural dependent persulfate activation by coke powder for aniline degradation. *Chemical Engineering Journal* **431**, 134088.

Zhou, P., Zhang, J., Zhang, Y., Zhang, G., Li, W., Wei, C., Liang, J., Liu, Y. & Shu, S. 2018 Degradation of 2,4-dichlorophenol by activating persulfate and peroxomonosulfate using micron or nanoscale zero-valent copper. *Journal of Hazardous Materials* **344**, 1209–1219.

Zhou, Z., Huang, J., Xu, Z., Ali, M., Shan, A., Fu, R. & Lyu, S. 2021 Mechanism of contaminants degradation in aqueous solution by persulfate in different Fe(II)-based synergistic activation environments: taking chlorinated organic compounds and benzene series as the targets. *Separation and Purification Technology* **273**, 118990.

Zhu, F., Li, L., Ma, S. & Shang, Z. 2016 Effect factors, kinetics and thermodynamics of remediation in the chromium contaminated soils by nanoscale zero valent Fe/Cu bimetallic particles. *Chemical Engineering Journal* **302**, 663–669.

Zhu, F., Li, L., Ren, W., Deng, X. & Liu, T. 2017 Effect of pH, temperature, humic acid and coexisting anions on reduction of Cr(VI) in the soil leachate by nZVI/Ni bimetal material. *Environmental Pollution* **227**, 444–450.

Zhu, C., Zhu, F., Dionysiou, D. D., Zhou, D., Fang, G. & Gao, J. 2018a Contribution of alcohol radicals to contaminant degradation in quenching studies of persulfate activation process. *Water Research* **139**, 66–73.

Zhu, F., He, S. & Liu, T. 2018b Effect of pH, temperature and co-existing anions on the removal of Cr(VI) in groundwater by green synthesized nZVI/Ni. *Ecotoxicology and Environmental Safety* **163**, 544–550.

Zhu, F., Ma, S., Liu, T. & Deng, X. 2018c Green synthesis of nano zero-valent iron/Cu by green tea to remove hexavalent chromium from groundwater. *Journal of Cleaner Production* **174**, 184–190.

Zhu, S., Li, X., Kang, J., Duan, X. & Wang, S. 2019 Persulfate activation on crystallographic manganese oxides: mechanism of singlet oxygen evolution for nonradical selective degradation of aqueous contaminants. *Environmental Science & Technology* **53**, 307–315.

Zhu, F., Wu, Y., Liang, Y., Li, H. & Liang, W. 2020 Degradation mechanism of norfloxacin in water using persulfate activated by BC@nZVI/Ni. *Chemical Engineering Journal* **389**, 124276.

Zhu, F., Zhou, S., Sun, M., Ma, J., Zhang, W., Li, K., Cheng, H. & Komarneni, S. 2022 Heterogeneous activation of persulfate by Mg doped $Ni(OH)_2$ for efficient degradation of phenol. *Chemosphere* **286**, 131647.

Zong, Y., Guan, X., Xu, J., Feng, Y., Mao, Y., Xu, L., Chu, H. & Wu, D. 2020 Unraveling the overlooked involvement of high-valent Cobalt-Oxo species generated from the cobalt(II)-activated peroxymonosulfate process. *Environmental Science & Technology* **54**, 16231–16239.

First received 15 November 2022; accepted in revised form 5 January 2023. Available online 19 January 2023